Prolactin-mediates a lactation-induced suppression of arcuate kisspeptin neuronal activity necessary for lactational infertility in mice

Eleni C.R. Hackwell[1,2], Sharon R. Ladyman[1,2,4], Jenny Clarkson[1,3], H. James McQuillan[1,2], Ulrich Boehm[5], Allan E. Herbison[6], Rosemary S.E. Brown[1,3], David R. Grattan[1,2,4]

[1]Centre for Neuroendocrinology, [2]Department of Anatomy and [3]Department of Physiology, School of Biomedical Sciences, University of Otago, Dunedin, NZ; [4]Maurice Wilkins Centre for Molecular Biodiscovery, Auckland, NZ; [5]Saarland University School of Medicine, Centre for Molecular Signalling (PZMS), Experimental Pharmacology, Homburg, Germany; [6]Department of Physiology, Development and Neuroscience, University of Cambridge, Cambridge, United Kingdom.

Corresponding author: David R. Grattan

Email: dave.grattan@otago.ac.nz

Author Contributions:

ECRH: Designed research, completed research, analysed data, wrote the first draft of the manuscript, edited the manuscript.
SRL: Designed research, completed research, analysed data, edited the manuscript.
JC: Completed research, analysed data, edited the manuscript.
HJM: Completed research, edited the manuscript.
UB: Provided key resources, edited the manuscript.
AEH: Designed research, analysed data, edited the manuscript.
RSEB: Designed research, analysed data, edited the manuscript.
DRG: Designed research, provided key resources, analysed data, edited the manuscript.

Competing Interest Statement: The authors have no competing interests to declare.

Abstract

The specific role that prolactin plays in lactational infertility, as distinct from other suckling or metabolic cues, remains unresolved. Here, deletion of the prolactin receptor (Prlr) from forebrain neurons or arcuate kisspeptin neurons resulted in failure to maintain normal lactation-induced suppression of estrous cycles. Kisspeptin immunoreactivity and pulsatile LH secretion were increased in these mice, even in the presence of ongoing suckling stimulation and lactation. GCaMP6 fibre photometry of arcuate kisspeptin neurons revealed that the normal episodic activity of these neurons is rapidly suppressed in pregnancy and this was maintained throughout early lactation. Deletion of Prlr from arcuate kisspeptin neurons resulted in early reactivation of episodic activity of kisspeptin neurons prior to a premature return of reproductive cycles in early lactation. These observations show dynamic variation in arcuate kisspeptin neuronal activity associated with the hormonal changes of pregnancy and lactation, and provide direct evidence that prolactin action on arcuate kisspeptin neurons is necessary for suppressing fertility during lactation.

Introduction

In mammals, lactation is accompanied by a period of infertility. This adaptive change establishes appropriate birth spacing to enable maternal metabolic resources to be directed towards caring for the new-born offspring, rather than supporting another pregnancy [1]. Lactational infertility is characterized by a lactation-induced suppression of pulsatile luteinizing hormone (LH) secretion, and the temporary loss of the reproductive cycle (in rodents this is exhibited as an extended period of diestrus or anestrus) [2-5]. Lactation is also characterised by chronically elevated levels of the anterior pituitary hormone prolactin, which is essential for milk production and promotes adaptive changes in maternal physiology and behaviour [1, 2, 4, 5]. Despite hyperprolactinaemia being a well-recognized cause of infertility, the specific role that prolactin plays in lactational infertility, as distinct from other suckling- or metabolic-related cues, is currently unclear [4, 6].

Recent *in vivo* studies have confirmed that kisspeptin neurons in the arcuate nucleus of the hypothalamus are responsible for the periodic release of gonadotrophin-releasing hormone (GnRH) and subsequent pulsatile luteinising hormone (LH) secretion that drives reproductive function [7-11]. Studies using GCaMP6 fibre photometry in conscious mice have demonstrated that the arcuate kisspeptin neuronal population exhibits episodes of increased intracellular calcium levels coincident with, and immediately preceding, each pulse of LH secretion in intact and gonadectomised male and female mice [7, 8 9]. Miniscope investigation showed that individual kisspeptin neurons within the arcuate population act in a coordinated, synchronised, and episodic manner [10, 11]. Loss of pulsatile LH secretion during lactation and consequent lactational infertility may be caused by the loss of kisspeptin-mediated stimulation of GnRH secretion [12-18]. Kisspeptin expression is markedly suppressed in lactation [12, 16] and when exogenously stimulated, kisspeptin neurons are unable to activate GnRH neurons during lactation, likely due to a lack of kisspeptin synthesis [13].

It is well established that hyperprolactinemia causes infertility, and thus, the elevated prolactin present in lactation seems a likely candidate to be involved in suppressing fertility during lactation. Prolactin administration acutely suppresses LH secretion [19], and chronic exposure to elevated prolactin reduces *Kiss1* mRNA expression in the arcuate nucleus [17, 20, 21]. In lactating mice, suppressing endogenous prolactin secretion shortens the period of infertility [22], suggesting that prolactin is important for maintaining the suppression of pulsatile LH secretion during lactation. Such a role for prolactin is controversial [4, 6, 23-27],

however, with studies in a number of species suggesting that the neural stimulation of suckling may be more important in maintaining lactational infertility [28, 29]. However, it has previously been difficult to disentangle the specific role of prolactin, as suckling, prolactin, and milk production are so tightly linked that manipulating one ultimately impacts the others, making it difficult to determine the contribution of any one element. Here, using a conditional deletion strategy, we have blocked prolactin action in the brain leaving suckling, lactation, and maternal behaviour intact. Using GCaMP fibre photometry techniques, we have also documented arcuate kisspeptin neuron activity across pregnancy and lactation transitions in the same mice and established that prolactin directly acts on these neurons to suppress fertility in lactation.

Materials and Methods

Animals

All experiments were performed using adult female mice on a C57BL/6J background (8-20 weeks of age). Mice were housed under controlled temperature (22 °C ± 2°C) and lighting (12-hour light/12-hour dark schedule, with lights on at 0600 hours) with *ad libitum* access to food and water (Teklad Global 18% Protein Rodent Diet 2918; Envigo, Huntingdon, United Kingdom). Daily body weight was recorded and vaginal cytology was used to monitor the estrous cycle stage. All experiments were carried out with approval from the University of Otago Animal Welfare and Ethics Committee.

Mice were mated with male wild-type C57BL/6J mice (presence of sperm plug = day 1 pregnancy). The first day a litter was seen was counted as day 1 of lactation and maternal mice were left undisturbed till day 3 of lactation, when vaginal monitoring would resume and litter size was normalised to 6 pups per animal, unless otherwise stated.

To monitor pulsatile secretion of LH, serial tail tip blood sampling and measurement of LH by ELISA was undertaken as reported previously [19, 30, 31]. As novel exposure and restraint stress has been shown to suppress pulsatile LH secretion [32], all mice were habituated to the tail tip blood sampling procedure in a gentle restraint device (soft cardboard tube) or hand, for at least 3 weeks prior to experimentation [33]. Sequential whole blood samples (4µl) were collected in 6 minute intervals for 3 hours between 0900 and 1200 hours unless otherwise stated. Samples were immediately diluted in 48ul 0.01M PBS/0.05% Tween 20, and frozen on dry ice before being stored at -20°C for subsequent LH measurement.

Effect of neuron-specific deletion of the prolactin receptor gene on the maintenance of lactational infertility

To investigate whether prolactin action in the brain is required for lactational infertility, neuron-specific *Prlr* knockout mice ($Prlr^{lox/lox}$/$Camk2a^{Cre}$) and their respective Cre-negative controls ($Prlr^{lox/lox}$) were generated, as previously described [34]. We have previously shown that while $Prlr^{lox/lox}$/$Camk2a^{Cre}$ mice do not have a complete Prlr deletion in the forebrain, there are areas of extensive deletion (as measured by reduced prolactin-induced pSTAT5), such as the arcuate nucleus and ventromedial nucleus of the hypothalamus, and areas where Prlr is reduced by about 50% such as the medial pre-optic area [34, 35]. RNAscope in-situ

hybridization was done to confirm knockdown. Briefly, intact diestrous mice and 14 day OVX mice (all aged 8-16 weeks) were perfused with 2% PFA to enable visualisation of kisspeptin cell bodies in both the RP3V and ARC regions (as kisspeptin cell bodies are only visible in the RP3V of intact mice and in the ARC of OVX mice, due to estradiol regulation [36]). Brain sections (14µm-thick) were prepared, thaw mounted onto superfrost-plus microscope slides and then stored at -80°C. RNAscope in-situ hybridization was performed using the RNAscope 2.5 High definition Duplex Detection kit – chromogenic (Advanced Cell Diagnostics, Hayward, CA) largely in accordance with manufacturer's instruction. The channel 1 Prlr probe was custom designed to pick up only the long form of the prolactin receptor. It was designed to transcript NM_011169.5 with a target sequence spanning nucleotides 1107-2147 (Ref: 588621; Advanced Cell Diagnostics, Hayward, CA). The channel 2 Kiss1 probe was custom designed to transcript NM_178260.3 with a target sequence spanning nucleotides 5 to 485 (Ref: 500141-C2; Advanced Cell Diagnostics, Hayward, CA). Sections were thawed at 55°C, postfixed for 3 minutes in 2% PFA, washed in 0.01M PBS for 5 minutes, and endogenous peroxidases were blocked with a hydrogen peroxidase solution for 10 minutes. Tissue was washed in distilled water (dH2O) (3x 2 minutes), then immersed in 100% ethanol briefly, air dried for 5 minutes, and a hydrophobic barrier was applied. Tissue was permeabilized with RNAscope protease plus for 30 minutes at 40°C. Sections were washed (2x 2 minutes) and were hybridized with the Prlr and Kiss1 probes (1:300 dilution, Prlr:Kiss1) or negative control probe (Cat#320751; Advanced Cell Diagnostics, Hayward, CA) at 40°C for 2 hours. Amplification (Amp 1-6) was performed in accordance with the manufacturer's instructions. Sections were then hybridized with a Fast-RED (1:60, Fast-RED B:Fast-RED A) for 10 minutes at room temperature, before undergoing further amplification steps (Amp 7-10) in accordance to manufacturer's instructions. The final positive hybridization was detected by incubation with the secondary detection reagents (1:50, Fast-GREEN B:Fast-GREEN) for 10 minutes at room temperature. Sections were washed, counterstained with haematoxylin (25% Gills), dried at 60°C for 20 minutes, and cover-slipped with VectaMount (Vector laboratories, H-5000) before imaging as previously described. Quantification of the proportion of kisspeptin neurons co-expressing *Prlr* mRNA was undertaken in FIJI software (National Institute of Health, Bethesda, Maryland, USA) following image acquisition. The total number of *Kiss1*-expressing cells and the total number of these that showed *Prlr* mRNA expression were counted.

$Prlr^{lox/lox}/Camk2a^{Cre}$ mice showed a significant decrease in the percentage of *Kiss1*-expressing cells co-expressing *Prlr* compared to controls in both the RP3V ($p = <0.0001$) and

arcuate nucleus (p = 0.0009) (unpaired two-tailed t tests, Supplementary Figure 1A-D). The *Prlr*$^{lox/lox}$/*Camk2a*^{Cre} mice are hyperprolactinaemic due to impaired negative feedback of prolactin on hypothalamic dopamine neurons [34] and therefore show disrupted estrous cycles (showing recurrent pseudopregnancy-like cycles with long periods of diestrus of approximately 14 days between estrus stages). However, these mice are able to become pregnant and have normal pregnancies. All mice were given a 250µl subcutaneous injection of bromocriptine (5mg/kg, 5% ethanol/saline; Tocris Bioscience Cat#0427) prior to being mated. This treatment was designed to reinstate an estrous cycle in *Prlr*$^{lox/lox}$/*Camk2a*^{Cre} mice. Bromocriptine is an agonist for the type 2 dopamine receptor and inhibits prolactin secretion from the pituitary gland [37], thereby terminating the pseudopregnancy-like state and bringing the mice into proestrus the following day. Following treatment, all mice were then housed with a stud male.

For *Prlr*$^{lox/lox}$/*Camk2a*^{Cre} mice, estrous cycles were monitored from day 3 of lactation until the first day of diestrus following a day of estrus (proestrus and estrus had to be observed prior to transcardial perfusion on the first day of diestrus). Brains were collected following transcardial perfusion for assessment of kisspeptin immunoreactivity. For every lactating *Prlr*$^{lox/lox}$/*Camk2a*^{Cre} mouse (n = 8), the brain of a *Prlr*$^{lox/lox}$ control mouse (n = 8) of the equivalent day (±1) of lactation was also collected. A group of non-lactating (NL) mice of both genotypes (n = 5-6) was also perfused for immunohistochemistry on diestrus.

To evaluate pulsatile LH secretion in early lactation (prior to the return of estrous cycles) and to determine whether progesterone played any role in regulating pulsatile LH secretion in lactation, additional groups of lactating *Prlr*$^{lox/lox}$/*Camk2a*^{Cre} and *Prlr*$^{lox/lox}$ control mice were generated and treated with either the progesterone receptor antagonist, mifepristone (4mg/kg in sesame oil, s.c.; AK Scientific Inc Cat#J10622), or vehicle (n = 7-8 per group) on the morning of day 4 of lactation and on day 5 of lactation, 30 minutes prior to blood sampling that day. This dose was selected as it was found to be sufficient to cause termination of pregnancy in wild-type C57BL/6J mice (p = 0.0072, Chi-squared test, Supplementary Figure 2A; pilot study) and neither vehicle nor mifepristone treatment had an effect on litter weight gain (interaction of time x genotype & treatment p = 0.5322, two-way repeated measures ANOVA, Supplementary Figure 2B).

Measurement of LH concentrations

An established sandwich ELISA method was used to determine LH concentration in diluted whole blood samples collected from mice [30, 31]. Briefly, a 96-well high plate was incubated with bovine monoclonal antibody (LHβ518b7, 1:1000 in 1xPBS; Dr. L. Sibley, UC Davis, CA, USA) for 16 h at 4°C. Following incubation of standards, controls and experimental samples for 2 hours, plates were incubated in rabbit polyclonal LH antibody (AFP240580Rb; 1:10,000; National Hormone and Pituitary Program, NIH) for 90 minutes, followed by incubation with polyclonal goat anti-rabbit IgG/HRP antibody (1:1000; DAKO Cytomation) for 90 minutes. Finally, plates were incubated in OPD (o-phenylenediamine capsules; Sigma-Aldrich Cat#P7288) for 30 minutes. A standard curve for the detection of LH concentration was generated using serial dilutions of mouse LH-reference preparation peptide (National Hormone and Pituitary Program, NIH). Luteinizing hormone levels were read using a standard absorbance plate reader (SpectraMax ABS Plus; Molecular Devices) at 490nm and 630nm wavelengths.

PULSAR Otago was used to define LH pulses [38]. Parameters used; Smoothing 0.7, Peak split 2.5, Level of detection 0.04, Amplitude distance 3, Assay variability 0, 2.5, 3.3, G(1)=3.5, G(2)=2.6, G(3)=1.9, G(4)=1.5, G(6)=1.2. Mean LH levels were calculated by averaging all LH levels collected during the experiment. The assay had a sensitivity of 0.04ng/ml to 4ng/ml, with an intra-assay coefficient of variation of 4.40% and an inter-assay coefficient of variation of 8.29%. See supplementary information, figure 1, for all individual LH profiles.

Assessment of kisspeptin expression

Perfusion and fixation of tissue

Mice were anaesthetised with sodium pentobarbital (15mg/mL) and transcardially perfused with 4% paraformaldehyde. Brains were removed, postfixed in the same solution, and cryoprotected overnight in 30% sucrose before being frozen at -80°C. Two sets of 30µm thick coronal brain sections were cut using a sliding microtome, from Bregma 1.10mm to -2.80mm. Brain sections were kept in cryoprotectant solution (pH = 7.6) at -20°C until immunohistochemistry was performed.

Immunohistochemistry

Immunohistochemistry for kisspeptin in the RP3V and arcuate nucleus was performed as previously described [39]. Briefly, sections were incubated in polyclonal rabbit anti-kisspeptin

primary antibody (AC 566, 1:10,000; gift from A. Caraty, Institut National de la Recherche Agronomique, Paris, France) for 48 hours at 4°C. Sections were then incubated with biotinylated goat anti-rabbit IgG (1:200, Vector biolabs, Peterborough, GK) for 90 min at room temperature, followed by incubation in an avidin-biotin complex (Elite vectastain ABC kit, Vector laboratories). The bound antibody-peroxidase complex was visualised using a nickel-enhanced diaminobenzidine (DAB) reaction, to form a black cytoplasmic precipitate.

Brain sections were imaged using an Olympus BX51 light microscope and Olympus UPlanSApo 10/20x lenses. Quantification of kisspeptin neurons in the RP3V, was undertaken by manually counting all labelled neurons present in all three subdivisions, the anteroventral periventricular nucleus (AVPV), rostral preoptic periventricular nucleus (rPVpo), and caudal preoptic periventricular nucleus (cPVpo, bregma 0.02) (2 sections per brain region per mouse) and then averaging this for each animal. As kisspeptin cell bodies in the arcuate nucleus were not easily observed, as previously reported [40], kisspeptin fibre immunoreactivity was imaged using a Gryphax NAOS colour camera (Jenoptik) and evaluated using FIJI software and the voxel counter function (National Institutes of Health). Kisspeptin fibre density was measured in the arcuate nucleus across the three subdivisions; rostral arcuate (rARC), middle arcuate (mARC), and caudal arcuate (cARC) with two sections of each area per animal counted, and then averaged across each animal to get total number and reported as total amount of voxels per ROI (voxel fraction).

Characterization of arcuate kisspeptin neuronal activity using GCaMP fibre photometry

Stereotaxic surgery and AAV injections

Adult *Kiss1*^{Cre} or *Prlr*$^{lox/lox}$/*Kiss1*^{Cre} mice (2-3 months old) were anaesthetised with 2% Isoflurane, given local Lidocaine (4mg/kg, s.c.) and Carprofen (5mg/kg, s.c.) and placed in a stereotaxic apparatus. A custom-made unilateral Hamilton syringe apparatus holding one Hamilton syringe was used to perform unilateral injections into the arcuate nucleus. The needles were lowered into place (-0.14mm A/P, +0.04mm M/L, -0.56mm DV) over 2 minutes and left in situ for 3 minutes before injection was made. 1µl AAV9-CAG-FLEX-GCaMP6s-WPRE-SV40 ($1.3x10^{-13}$ GC/ml, University of Pennsylvania Vector Core, Philadelphia, PA, USA) was injected into the arcuate nucleus at a rate of ~100nl/min with the needles left in situ for 3 minutes prior to being withdrawn over a period of 6 minutes. This

was followed by implantation of a unilateral indwelling optical fibre (400 µm diameter, 6.5 mm long, 0.48 numerical aperture (NA), Doric Lenses, Canada, product code: MFC_400/430-0.48_6.5mm_SM3*_FLT) at the same coordinates. Carprofen (5mg/kg body weight, s.c.) was administered for post-operative pain relief. After surgery, mice received daily handling and habituation to the photometry recording procedure over 4-6 weeks before experimentation began.

GCaMP6 fibre photometry

Photometry was performed as reported previously [9]. Fluorescence signals were acquired using a custom-built fibre photometry system made primarily from Doric components. Violet (405nm) and blue (490nm) fibre-coupled LEDs were sinusoidally modulated at 531 and 211 Hz, respectively, and focused into a 400µm, 0.48 numerical aperture fibre optic patch cord connected to the mouse. Emitted fluorescence was collected by the same fibre and focused onto a femtowatt photoreceiver (2151, Newport). The two GCaMP6s emission signals were collected at 10 Hz in a scheduled 5s on/15s off mode by demodulating the 405nm (non-calcium dependent) and 490nm (calcium dependent) signals. The power output at the tip of the fibre was set at 50µW. Fluorescent signals were acquired using a custom software acquisition system (Tussock Innovation, Dunedin, New Zealand) and analysed using custom templates created by Dr Joon Kim (University of Otago, Dunedin, New Zealand) based on mathematics and calculations similar to those previously described [41, 42]. Briefly, the fluorescent signal obtained after stimulation with 405nm light was used to correct for movement artefacts as follows: first, the 405nm signal was filtered using a savitzky-golay filter and fitted to the 490nm signal using least linear square regression. The fitted 405nm signal was then subtracted and divided from the 490nm signal to obtain the movement and bleaching corrected signal. The output of these templates is 490- adjusted405/adjusted405, which was multiplied to get the final ΔF/F as a percentage increase (all photometry data reported as ΔF/F(%)).

All recordings were obtained from freely behaving mice for up to 24 hours and occurred between the hours of 0800 hours and 1200 hours (apart from 24 hours post weaning recording (0900 hours to 1700 hours), and day 18/19 pregnancy recording (1800 hours to 0800 hours the following day). Synchronized events (SE) were defined as when ΔF/F exceeds 3 standard deviations (SD) above the trace mean. Manual event shape analysis was performed in addition to standard deviation method for certain datasets where necessary.

Events were counted manually to determine frequency of events per 60 minutes. The between animal variability in total signal means that changes in SE amplitude can only be reported as relative changes within an animal. Relative SE amplitude was calculated by using normalised ΔF/F data and then subtracting the peak of an SE from the nearest nadir to the rise of the SE and averaging that for the number of SEs in a recording. To obtain normalised ΔF/F, three pre-pregnancy datasets from each mouse were used to find the average maximum ΔF/F for that mouse. All datasets were then divided by that normalisation value to get normalised ΔF/F for each trace for each individual mouse.

Monitoring the activity of arcuate kisspeptin neurons across different reproductive stages in the same mice

Adult *Kiss1*^{Cre} mice were 8-10 weeks of age at the beginning of experiments, and up to 12 months in age by time of final recording (n = 8 during pregnancy, n = 6 during lactation; 2 mice were euthanised due to dystocia therefore those mice were only followed through pregnancy). Monitoring of vaginal cytology and weights was continuous from 1 week pre-surgery till day 19 of pregnancy and resumed on day 3 of lactation (with all handling stopped on day 19 to avoid potential compromise of parturition and onset of maternal behaviour). To investigate the activity of the arcuate kisspeptin population across different reproductive states in the same animal, the following recording protocol was followed for all *Kiss1*^{Cre} mice, unless otherwise stated; virgin (diestrus), day 4 of pregnancy, day 14 of pregnancy, day 18/19 of pregnancy (overnight), day 7 of lactation, day 14 of lactation, day 18 of lactation, 24 hours after weaning, first diestrus after estrous cycles begin following weaning, and 10 days after OVX. In addition, blood sample collection for paired LH measurement was done in virgin (diestrus) state, on day 14 of pregnancy (in 4 mice, maximum of 6 samples were collected around small "peaks" in baseline), day 7 of lactation, and day 14 of lactation. Blood sampling was not carried out at additional time points as blood sampling was undertaken at least a week apart, and stress from repeated sampling was attempted to be kept at a minimum e.g., not blood sampling around the time of birth. Fibre photometry recordings were usually between 2-4 hours in length. The only longer recordings were undertaken on day 18/19 of pregnancy (14 hours) and 24 hours after weaning (8 hours). These particular recording sessions were extended to determine whether there were any longer-term changes occurring in the activity of the arcuate kisspeptin population in the lead up to parturition or following

weaning of pups (states closely followed by postpartum estrus and resumption of normal estrous cycles, respectively).

Effect of arcuate kisspeptin neuron-specific deletion of the prolactin receptor gene on the maintenance of lactational infertility and the activity of kisspeptin neurons during lactation

Kisspeptin-specific prolactin-receptor knockout mice (*Prlr*$^{lox/lox}$/*Kiss1*$^{Cre\ 19}$) and their respective Cre-negative controls (*Prlr*$^{lox/lox}$) were generated. RNAscope in-situ hybridization was done to confirm knockdown, with *Prlr*$^{lox/lox}$/*Kiss1*^{Cre} mice showing a significant decrease in the percentage of *Kiss1*-expressing cells co-expressing *Prlr* compared to controls in the arcuate ($p = <0.0001$, unpaired two-tailed t test, Extended data Figure 3E, F). Similar to experiments described above, *Prlr*$^{lox/lox}$/*Kiss1*^{Cre} (n = 27) and *Prlr*$^{lox/lox}$ control (n = 30) dams underwent estrous cycle monitoring from day 3 of lactation onwards to determine whether mice showed an early resumption of estrus cycles.

To determine whether the deletion of the prolactin receptor from arcuate kisspeptin neurons led to early reactivation of these neurons during lactation, adult *Prlr*$^{lox/lox}$/*Kiss1*^{Cre} mice (n = 5) and an additional *Kiss1*^{Cre} control mouse (n = 1) (8 weeks old at the start of the experiment, and up to 14 months at end of final recording timepoint) were set up for fibre photometry, as described above. Monitoring of vaginal cytology and weights was continuous from 1 week pre-surgery till day 18 of pregnancy and resumed on day 3 of lactation. Recordings were undertaken in a similar timeline as described above, however no pregnancy recordings were done, and in early lactation recordings were performed every 2 days from day 3 to day 9 of lactation, before following the same protocol as described. No blood samples were taken over this lactation period in this genotype. As described previously, recordings were kept between 2-4 hours, apart from the 24 hours after weaning recording (8 hours).

Statistical analysis

Data are presented as mean ± SEM and all statistical analysis was performed with PRISM software 10 (GraphPad Software, San Diego, CA, USA) with a p value of < 0.05 considered as statistically significant. Individual symbols in graphs represent individual mice. Differences in kisspeptin cells number or fibre density was assessed using two-way

335 ANOVAs with Tukey's multiple comparisons tests or t tests, with both analyses using
336 combined averages of each animal (averaged number of cells or fibre density across the three
337 subdivisions of each nucleus to get total number reported). Resumption of estrous cycles was
338 analysed using Log-rank (Mantel-Cox) test chi square test. LH pulse frequency data and
339 mean LH data was analysed using two-way ANOVAs with Tukey's multiple comparisons
340 tests. SE frequency and amplitude throughout reproductive cycles was analysed using mixed
341 effect analysis (fixed type III) with Tukey's multiple comparisons tests where appropriate
342 and day 18/19 of pregnancy data was analysed using t tests. Correlation between SE
343 occurrence and LH pulses was assessed using chi-square test. All fibre photometry data used
344 for quantitative analysis and comparison were from the first pregnancy and lactation. A full
345 list of probability values, inferential statistics, and degrees of freedom for all data can be
346 found in Supplementary Table 1.

347

Results

Prolactin action on forebrain neurons is necessary to maintain lactational infertility

Lactation has previously been associated with a marked decrease in *Kiss1* mRNA levels in both rostral periventricular region of the third ventricle (RP3V) and arcuate nucleus populations during lactation [13]. To determine whether prolactin is involved in the maintenance of lactational anestrus, the *Prlr* gene was knocked out of *Camk2a* expressing neurons (most forebrain neurons, as described in [34]) of female mice. Control $Prlr^{lox/lox}$ mice showed a marked reduction in kisspeptin cell body immunoreactivity in the RP3V of lactating compared to virgin mice ($p = 0.0100$, *Post hoc* Tukey's multiple comparisons test, Figure 1A, C). In contrast, lactation-induced suppression of kisspeptin cell bodies in the RP3V and fibre labelling in the arcuate nucleus was absent in $Prlr^{lox/lox}/Camk2a^{Cre}$ mice ($p = 0.6409$, *Post hoc* Tukey's multiple comparisons test, Figure 1A, C; interaction between reproductive state and genotype $p = 0.0034$, two-way ANOVA, Figure 1A, C; $p = 0.0020$, unpaired two tailed t test, measured as percentage voxels within the region of interest, Figure 1B, D).

Estrous cycles during lactation were significantly altered by deletion of Prlr in the forebrain, with all $Prlr^{lox/lox}/Camk2a^{Cre}$ mice showing a return to estrus between day 6 and day 10 of lactation (Figure 1E), while, as normal, estrus did not occur until day 20 in control $Prlr^{lox/lox}$ mice ($p = <0.0001$, log-rank (Mantel-Cox) test, Figure 1E). No differences in litter weight gain from day 3 to day 8 of lactation were observed in either group ($p = 0.3282$, mixed analysis test, Supplementary Figure 3), indicating that the suckling stimulus that mice received was maintained in the absence of *Prlr* expression in *Camk2a* expressing neurons. Collectively, these data show that prolactin action in the brain is absolutely required for the lactation-induced suppression of kisspeptin expression and to maintain lactational infertility in mice.

In a separate cohort of mice, pulsatile LH secretion in $Prlr^{lox/lox}/Camk2a^{Cre}$ mice was monitored in early lactation, prior to the return of estrous cycles. To rule out a potential role for progesterone in suppressing fertility during lactation [9, 43, 44], the progesterone receptor antagonist mifepristone (RU486), was administered to mice in early lactation. Vehicle-treated $Prlr^{lox/lox}$ control mice showed the expected near complete absence of pulsatile LH secretion during lactation (Figure 2A, B). In contrast, nearly all $Prlr^{lox/lox}/Camk2a^{Cre}$ mice showed a

lack of the normal lactation-induced suppression of pulsatile LH secretion demonstrated by a significant increase in frequency of LH pulses compared to controls (effect of genotype p = 0.0024, two-way ANOVA with Tukey's multiple comparisons test, Figure 2A, B). There was no effect of mifepristone on this pattern of LH secretion, suggesting that progesterone action is not required for the suppression of LH secretion (LH pulse frequency (interaction genotype x treatment p = 0.2807; treatment p = 0.8588; Figure 2B), mean LH levels (interaction genotype x treatment p = 0.8697; treatment p = 0.8586; Figure 2C), two-way ANOVA with Tukey's multiple comparisons test). These data indicate that prolactin is the primary signal responsible for the suppression of LH during lactation in mice. Individual LH profiles from all animals are shown in Supplementary Figure 4.

Episodic activity of arcuate kisspeptin neurons is suppressed during pregnancy and most of lactation

To directly assess the role of prolactin in regulating kisspeptin neuron activity during lactation, GCaMP6 fibre photometry was undertaken to monitor real-time activity of arcuate kisspeptin neurons in freely behaving mice. We first undertook a longitudinal assessment of changes in kisspeptin neuronal activity by tracking individual animals throughout pregnancy and lactation and following weaning (Figure 3).

Initially, GCaMP fibre photometry recordings were collected in the virgin diestrous state, both with and without serial blood sampling to measure LH concentrations. As can be seen in Figure 4A, photometry recordings were characterized by discrete synchronised events (SEs) of elevated intracellular calcium (indicative of synchronous activity of the kisspeptin population), with each SE correlating perfectly to a single pulse of LH in the minutes following (p = <0.0001, chi-squared test). These were observed to be at a similar rate to that described previously in diestrous mice using GCaMP photometry in a different *Kiss1* mouse line [9], with periodic SEs occurring about once per hour (1.250±0.250; Figure 3 & 4B).

The activity of the arcuate kisspeptin population in *Kiss1*^{Cre} mice dynamically changed depending on the reproductive state of the mouse (p = 0.0012, mixed-effect analysis, Figure 3 & 4B). On day 4 of pregnancy, SE frequency had markedly decreased (0.297±0.136/hr; Figure 3 & 4B), indicating an early reduction in activity of arcuate kisspeptin neurons during pregnancy. By day 14 of pregnancy, no SEs were seen (0±0/hr; Figure 3 & 4B) and this was confirmed by a lack of pulsatile LH secretion (Supplementary Figure 5). In late pregnancy

(day 18), neuronal activity was monitored for 14 hours, during which time low amplitude, SEs were unexpectedly observed at similar frequencies to virgin levels (2.043±0.940/hr; Figure 3 & 4B-C). This unusual pattern of activity is illustrated in more detail in Figure 5 where alongside the resurgence of low amplitude SEs, there was a marked increase in baseline activity observed, relative to other stages. This activity was reminiscent of the miniature SEs observed to be caused by activation of subgroups of cells in a brain slice technique [11], but we are unable to resolve such events using the present methods. Since our aim was to continue longitudinal assessment of the arcuate kisspeptin population into lactation and weaning, mice were not disrupted by blood sampling immediately prior to parturition as we were concerned that this additional stressor might interfere with establishment of maternal behaviour. Hence, we are unable to report whether these low amplitude SEs and elevated baseline activity were associated with LH secretion.

Evaluation of activity of arcuate kisspeptin neurons during lactation showed complete suppression of activity on day 7 of lactation with a corresponding absence of pulsatile LH secretion (0±0/hr; Figure 3 & 4B). This lactation-induced suppression of activity was partially relieved by day 14 of lactation (0.583±0.083/hr; Figure 3 & 4B), with SEs again corresponding to low frequency pulses of LH secretion. Further increases in SE frequency were seen on day 18 of lactation (0.850±0.100/hr; Figure 3 & 4B), including an increase in baseline activity, similar to that seen in late pregnancy, and by 24 hours after weaning (day 22 postpartum) the frequency of SEs returned to close to non-pregnant levels (1.375±0.114/hr; Figure 3 & 4B). Frequency remained unchanged on the day of first diestrus following a return to estrous cycles after weaning (1.533±0.226/hr; Figure 3 & 4B). As a final manipulation, mice were ovariectomized (OVX), and arcuate kisspeptin population activity observed to increase significantly with clusters of high amplitude activity (4.778±0.222/hr; Figure 3 & 4B), consistent with previous reports following OVX in nulliparous mice [45]. Collectively, these observations show extensive, dynamic variation in activity of the arcuate kisspeptin neuronal population associated with pregnancy and lactation.

Mice with an arcuate kisspeptin neuron-specific deletion have premature reactivation of estrous cycles and neuronal activity in lactation

To determine whether the prolactin-induced suppression of estrous cycles and LH pulsatile secretion was specifically mediated by kisspeptin neurons, mice were generated with an

arcuate-specific deletion of the Prlr from kisspeptin neurons [19]. Similar to the data from forebrain neuron-specific deletion of Prlr, there was early resumption of estrous cycles in *Prlr*$^{lox/lox}$/*Kiss1*^{Cre} mice during lactation (63% showing estrus by day 10 of lactation and 83% by day 19 lactation) compared to *Prlr*$^{lox/lox}$ controls (4% by day 19 lactation) ($p = <0.0001$, log-rank (Mantel-Cox) test, Figure 6A). No difference in litter weight gain during lactation (day 3-20 of lactation weight gain) was observed in either group ($p = 0.6404$, two-way ANOVA, Supplementary Figure 1H) indicating that suckling and/or lactation itself was not impaired. *In vivo* GCaMP6 fibre photometry in *Prlr*$^{lox/lox}$/*Kiss1*^{Cre} mice showed early reactivation of the arcuate kisspeptin population between day 3 and 5 of lactation (Figure 6C). This was accompanied by a clear return to estrous within this early lactation window in 4/5 mice. These data demonstrate that prolactin action specifically on arcuate kisspeptin neurons is responsible for maintaining suppression of those neurons, and thereby fertility, during lactation in mice.

Discussion

We demonstrate here that prolactin action in arcuate kisspeptin neurons is necessary for the maintained suppression of fertility during lactation in mice. Neuron-specific Prlr deletion (*Prlr*$^{lox/lox}$/*Camk2a*^{Cre}) resulted in premature return to estrus in early lactation, even in the presence of ongoing suckling stimulus and the full metabolic consequences of milk production. Accompanying the resumption of estrus was an absence of the normal lactation-induced reduction in kisspeptin immunoreactivity [12, 16, 20], and pulsatile LH secretion was also observed on day 5 of lactation prior to the premature estrus when it would normally have been completely absent [46-48]. To evaluate the specific role of kisspeptin neurons in mediating the prolactin-induced suppression of fertility, we have comprehensively mapped the activity of arcuate kisspeptin neurons throughout a full reproductive cycle: pregnancy, lactation, and after weaning in individual animals. The data show an immediate suppression of activity of arcuate kisspeptin neuronal activity during pregnancy, and this is maintained throughout most of lactation, apart from a brief window of reactivation immediately prior to parturition. Deleting Prlr specifically from arcuate kisspeptin neurons prevented the suppression of activity in early lactation, resulting in premature induction of episodic activation of kisspeptin neurons, and early onset of estrus. Combined, these data provide direct evidence that prolactin action on kisspeptin neurons is necessary for lactation-induced infertility in mice.

It is now well established that the arcuate kisspeptin neurons form the GnRH "pulse generator", and hence drive pulsatile release of GnRH from the hypothalamus and consequent pulses of LH form the pituitary that is required for fertility [49-51]. This is the first study to monitor activity of the GnRH "pulse generator" across different reproductive states in the same animal, and the data largely match previously described patterns of LH secretion [47, 52]. The frequency and dynamics of the synchronised events changed dramatically, initially due to the pregnancy-induced changes in ovarian hormones. The abrupt decrease in "pulse generator" activity in early gestation is likely caused by rising levels of progesterone, known to profoundly suppress activity of arcuate kisspeptin neurons and LH secretion [9, 43, 44]. Progesterone is elevated throughout pregnancy, gradually increasing until luteolysis and progesterone withdrawal occurs in the lead up to parturition [53-56]. Interestingly, we observed a transient reactivation of the arcuate kisspeptin neurons in the night between days 18 and 19 of pregnancy. This was characterised by frequent, low amplitude episodes of activity, and increased baseline activity that may represent the intermittent synchronized activity of small

subsets of arcuate kisspeptin neurons that have not yet transitioned to full synchronization of the whole population [11]. It seems likely that this pattern of activity is associated with progesterone withdrawal in late pregnancy and may be important in stimulating follicular growth leading up to a postpartum ovulation [57, 58].

In early lactation, episodic activity of arcuate kisspeptin neurons was absent, with sporadic low-amplitude activity returning around day 14 of lactation. There was another period of increased baseline activity in late lactation, similar to that seen in late pregnancy, potentially representing a signature of reactivation of synchronized activity of the arcuate kisspeptin neurons. Overall patterns of activity rapidly returned to normal diestrous levels soon after weaning. This increase in "pulse generator" activity during late lactation mirrors the increase in LH levels that has been reported as lactation progresses [59]. In the absence of Prlr in arcuate kisspeptin neurons, however, synchronized episodic activity re-appeared as early as 3 days after birth, even in the presence of ongoing suckling. These data clearly show that prolactin action in the arcuate kisspeptin neurons is necessary to sustain lactational infertility in mice. The observed disruption of lactational infertility in *Prlr*$^{lox/lox}$/*Kiss1*^{Cre} mice is particularly remarkable given that Prlr deletion is restricted to arcuate kisspeptin neurons in this model [19], and prolactin action on RP3V kisspeptin neurons [21, 60] and on gonadotrophs in the pituitary gland [61-63] are unaffected.

The indispensable role for prolactin in mediating lactation-induced infertility in the mouse is surprising, given the consensus of much work in other species concluding that other factors may be more important (see [4, 6, 26, 27, 64]). This may reflect a level of redundancy amongst contributing factors across all species, including ovarian hormones, metabolic cues and neural inputs of suckling. Notably, the conditional deletion approach described here distinguishes prolactin action from the neurogenic effects of suckling without altering the process of lactation itself. Moreover, this approach avoids the potential confounding effects of using dopamine agonists to suppress prolactin [28, 29], given that dopamine can directly inhibit GnRH neuronal activity [65].

While the effects of widespread neuronal deletion (*Prlr*$^{lox/lox}$/*Camk2a*^{Cre}) on fertility were largely recapitulated by the arcuate kisspeptin-specific model, it was apparent that the global deletion was more effective at inducing the return to estrus during lactation (in 100% of animals by day 10), compared to the arcuate kisspeptin-specific model (63% by day 10, and 83% by day 19). This may be due to the absence of lactation-induced suppression of *Kiss1*

519 expression in RP3V kisspeptin neurons of *Prlr*$^{lox/lox}$/*Camk2a*^{Cre} mice. Similarly, we cannot
520 rule out the possibility that other populations of prolactin-sensitive neurons, such as GABA
521 or dopamine neurons [60], may contribute to suppressing estrous cycles during lactation.
522 Nevertheless, our data collectively provide strong evidence that prolactin action on arcuate
523 kisspeptin neurons is the primary factor mediating lactation-induced infertility in mice. Given
524 that hyperprolactinemia induces infertility in humans and many other species [21, 22, 66-75], it is
525 likely that a conserved mechanism will be contributing to lactational infertility in all
526 mammalian species.

Acknowledgments

We would like to acknowledge the research assistance of Zin Khant-Aung, genotyping by Pene Knowles, and Dr Joon Kim for his assistance with analysis of fibre photometry data.

Financial support: This work was supported by Health Research Council of New Zealand (grant number: 21-560) and the Lions Club of Dunedin South - administered by Perpetual Guardian (Otago Medical Research Foundation).

References

1. Short, R.V. Lactation--the central control of reproduction. *Ciba Foundation symposium*, 73-86 (1976).
2. McNeilly, A.S.*, et al.* Fertility after childbirth: pregnancy associated with breast feeding. *Clin Endocrinol (Oxf)* **19**, 167-173 (1983).
3. Fox, S.R. & Smith, M.S. The suppression of pulsatile luteinizing hormone secretion during lactation in the rat. *Endocrinology* **115**, 2045-2051 (1984).
4. McNeilly, A.S. Lactational control of reproduction. *Reprod Fertil Dev* **13**, 583-590 (2001).
5. Tsukamura, H. & Maeda, K. Non-metabolic and metabolic factors causing lactational anestrus: rat models uncovering the neuroendocrine mechanism underlying the suckling-induced changes in the mother. *Progress in brain research* **133**, 187-205 (2001).
6. McNeilly, A.S. Lactation and fertility. *Journal of mammary gland biology and neoplasia* **2**, 291-298 (1997).
7. Clarkson, J.*, et al.* Definition of the hypothalamic GnRH pulse generator in mice. *Proc Natl Acad Sci U S A* **114**, E10216-E10223 (2017).
8. Han, S.Y., Kane, G., Cheong, I. & Herbison, A.E. Characterization of GnRH Pulse Generator Activity in Male Mice Using GCaMP Fiber Photometry. *Endocrinology* **160**, 557-567 (2019).
9. McQuillan, H.J., Han, S.Y., Cheong, I. & Herbison, A.E. GnRH Pulse Generator Activity Across the Estrous Cycle of Female Mice. *Endocrinology* **160**, 1480-1491 (2019).
10. Moore, A.M., Coolen, L.M. & Lehman, M.N. In vivo imaging of the GnRH pulse generator reveals a temporal order of neuronal activation and synchronization during each pulse. *Proceedings of the National Academy of Sciences* **119**, e2117767119 (2022).
11. Han, S.Y.*, et al.* Mechanism of kisspeptin neuron synchronization for pulsatile hormone secretion in male mice. *Cell Rep* **42**, 111914 (2023).
12. Yamada, S.*, et al.* Inhibition of metastin (kisspeptin-54)-GPR54 signaling in the arcuate nucleus-median eminence region during lactation in rats. *Endocrinology* **148**, 2226-2232 (2007).
13. Liu, X., Brown, R.S., Herbison, A.E. & Grattan, D.R. Lactational anovulation in mice results from a selective loss of kisspeptin input to GnRH neurons. *Endocrinology* **155**, 193-203 (2014).
14. Roa, J.*, et al.* Hypothalamic expression of KiSS-1 system and gonadotropin-releasing effects of kisspeptin in different reproductive states of the female Rat. *Endocrinology* **147**, 2864-2878 (2006).
15. Ladyman, S.R. & Woodside, B. Food restriction during lactation suppresses Kiss1 mRNA expression and kisspeptin-stimulated LH release in rats. *Reproduction* **147**, 743-751 (2014).
16. True, C., Kirigiti, M., Ciofi, P., Grove, K.L. & Smith, M.S. Characterisation of arcuate nucleus kisspeptin/neurokinin B neuronal projections and regulation during lactation in the rat. *J Neuroendocrinol* **23**, 52-64 (2011).
17. Brown, R.S., Herbison, A.E. & Grattan, D.R. Prolactin regulation of kisspeptin neurones in the mouse brain and its role in the lactation-induced suppression of kisspeptin expression. *J. Neuroendocrinol.* **26**, 898-908 (2014).
18. Xu, J., Kirigiti, M.A., Grove, K.L. & Smith, M.S. Regulation of food intake and gonadotropin-releasing hormone/luteinizing hormone during lactation: role of insulin and leptin. *Endocrinology* **150**, 4231-4240 (2009).

19. Brown, R.S.E., *et al.* Acute Suppression of LH Secretion by Prolactin in Female Mice Is Mediated by Kisspeptin Neurons in the Arcuate Nucleus. *Endocrinology* **160**, 1323-1332 (2019).
20. Araujo-Lopes, R., *et al.* Prolactin regulates kisspeptin neurons in the arcuate nucleus to suppress LH secretion in female rats. *Endocrinology* **155**, 1010-1020 (2014).
21. Sonigo, C., *et al.* Hyperprolactinemia-induced ovarian acyclicity is reversed by kisspeptin administration. *J Clin Invest* **122**, 3791-3795 (2012).
22. Hackwell, E.C., Ladyman, S.R., Brown, R.S. & Grattan, D.R. Mechanisms of lactation-induced infertility in female mice. *Endocrinology* **164**, bqad049 (2023).
23. Schallenberger, E., Richardson, D.W. & Knobil, E. Role of prolactin in the lactational amenorrhea of the rhesus monkey (Macaca mulatta). *Biol Reprod* **25**, 370-374 (1981).
24. McNeilly, A. Suckling and the control of gonadotropin secretion. in *The Physiology of Reproduction* (ed. J.N. E. Knobil) 1179–1212 (Raven Press, New York, 1994).
25. Sugimoto, A., *et al.* Central somatostatin-somatostatin receptor 2 signaling mediates lactational suppression of luteinizing hormone release via the inhibition of glutamatergic interneurons during late lactation in rats. *Journal of Reproduction and Development* (2022).
26. Tay, C.C., Glasier, A.F. & McNeilly, A.S. Twenty-four hour patterns of prolactin secretion during lactation and the relationship to suckling and the resumption of fertility in breast-feeding women. *Human reproduction (Oxford, England)* **11**, 950-955 (1996).
27. Diaz, S., *et al.* Circadian variation of basal plasma prolactin, prolactin response to suckling, and length of amenorrhea in nursing women. *The Journal of clinical endocrinology and metabolism* **68**, 946-955 (1989).
28. Maeda, K., *et al.* Prolactin does not mediate the suppressive effect of the suckling stimulus on luteinizing hormone secretion in ovariectomized lactating rats. *Endocrinologia japonica* **37**, 405-411 (1990).
29. Smith, M.S. The relative contribution of suckling and prolactin to the inhibition of gonadotropin secretion during lactation in the rat. *Biol Reprod* **19**, 77-83 (1978).
30. Steyn, F.J., *et al.* Development of a methodology for and assessment of pulsatile luteinizing hormone secretion in juvenile and adult male mice. *Endocrinology* **154**, 4939-4945 (2013).
31. Czieselsky, K., *et al.* Pulse and Surge Profiles of Luteinizing Hormone Secretion in the Mouse. *Endocrinology* **157**, 4794-4802 (2016).
32. Briski, K.P. & Sylvester, P.W. Effects of sequential acute stress exposure on stress-induced pituitary luteinizing hormone and prolactin secretion. *Life sciences* **41**, 1249-1255 (1987).
33. Steyn, F.J., *et al.* Development of a method for the determination of pulsatile growth hormone secretion in mice. *Endocrinology* **152**, 3165-3171 (2011).
34. Brown, R.S., *et al.* Conditional Deletion of the Prolactin Receptor Reveals Functional Subpopulations of Dopamine Neurons in the Arcuate Nucleus of the Hypothalamus. *J. Neurosci.* **36**, 9173-9185 (2016).
35. Gustafson, P., *et al.* Prolactin receptor-mediated activation of pSTAT5 in the pregnant mouse brain. *J Neuroendocrinol* **32**, e12901 (2020).
36. Smith, J.T., Cunningham, M.J., Rissman, E.F., Clifton, D.K. & Steiner, R.A. Regulation of Kiss1 gene expression in the brain of the female mouse. *Endocrinology* **146**, 3686-3692 (2005).
37. Moult, P.J., Rees, L.H. & Besser, G.M. Pulsatile gonadotrophin secretion in hyperprolactinaemic amenorrhoea an the response to bromocriptine therapy. *Clin Endocrinol (Oxf)* **16**, 153-162 (1982).

38. Porteous, R., *et al.* Reformulation of PULSAR for Analysis of Pulsatile LH Secretion and a Revised Model of Estrogen-Negative Feedback in Mice. *Endocrinology* **162** (2021).
39. Clarkson, J., d'Anglemont de Tassigny, X., Colledge, W.H., Caraty, A. & Herbison, A.E. Distribution of kisspeptin neurones in the adult female mouse brain. *J Neuroendocrinol* **21**, 673-682 (2009).
40. Clarkson, J., Boon, W.C., Simpson, E.R. & Herbison, A.E. Postnatal development of an estradiol-kisspeptin positive feedback mechanism implicated in puberty onset. *Endocrinology* **150**, 3214-3220 (2009).
41. Kim, C.K., *et al.* Simultaneous fast measurement of circuit dynamics at multiple sites across the mammalian brain. *Nature methods* **13**, 325-328 (2016).
42. Sherathiya, V.N., Schaid, M.D., Seiler, J.L., Lopez, G.C. & Lerner, T.N. GuPPy, a Python toolbox for the analysis of fiber photometry data. *Scientific Reports* **11**, 24212 (2021).
43. Goodman, R.L. & Karsch, F.J. Pulsatile secretion of luteinizing hormone: differential suppression by ovarian steroids. *Endocrinology* **107**, 1286-1290 (1980).
44. Skinner, D.C., *et al.* The negative feedback actions of progesterone on gonadotropin-releasing hormone secretion are transduced by the classical progesterone receptor. *Proc Natl Acad Sci U S A* **95**, 10978-10983 (1998).
45. McQuillan, H.J., *et al.* Definition of the estrogen negative feedback pathway controlling the GnRH pulse generator in female mice. *Nature Communications* **13**, 7433 (2022).
46. Bohnet, H.G. & Schneider, H.P. Prolactin as a cause of anovulation. in *Prolactin and human reproduction* (ed. P.G. Crosignani & C. Robyn) 153-159 (Academic Press, New York, 1977).
47. McNeilly. Effects of lactation on fertility. (1979).
48. McNeilly, A.S., Tay, C.C. & Glasier, A. Physiological mechanisms underlying lactational amenorrhea. *Ann. N. Y. Acad. Sci.* **709**, 145-155 (1994).
49. Herbison, A.E. The Gonadotropin-Releasing Hormone Pulse Generator. *Endocrinology* **159**, 3723-3736 (2018).
50. de Roux, N., *et al.* Hypogonadotropic hypogonadism due to loss of function of the KiSS1-derived peptide receptor GPR54. *Proc Natl Acad Sci U S A* **100**, 10972-10976 (2003).
51. Seminara et al. The GPR54 gene as a regulator of puberty. (2003).
52. Morishige, W.K., Pepe, G.J. & Rothchild, I. Serum luteinizing hormone, prolactin and progesterone levels during pregnancy in the rat. *Endocrinology* **92**, 1527-1530 (1973).
53. Virgo, B.B. & Bellward, G.D. Serum progesterone levels in the pregnant and postpartum laboratory mouse. *Endocrinology* **95**, 1486-1490 (1974).
54. Pointis, G., Rao, B., Latreille, M., Mignot, T.-M. & Cedard, L. Progesterone levels in the circulating blood of the ovarian and uterine veins during gestation in the mouse. *Biology of Reproduction* **24**, 801-805 (1981).
55. Bridges, R.S. A quantitative analysis of the roles of dosage, sequence, and duration of estradiol and progesterone exposure in the regulation of maternal behavior in the rat. *Endocrinology* **114**, 930-940 (1984).
56. Sugimoto, Y., *et al.* Failure of parturition in mice lacking the prostaglandin F receptor. *Science* **277**, 681-683 (1997).
57. Thapa, S., Short, R.V. & Potts, M. Breast feeding, birth spacing and their effects on child survival. *Nature* **335**, 679-682 (1988).
58. Zakar, T. & Hertelendy, F. Progesterone withdrawal: key to parturition. *American journal of obstetrics and gynecology* **196**, 289-296 (2007).

59. Rolland, R., Lequin, R.M., Schellekens, L.A. & Jong, F.H.D. The role of prolactin in the restoration of ovarian function during the early post-partum period in the human female: I. A study during physiological lactation. *Clinical Endocrinology* **4**, 15-25 (1975).
60. Kokay, I.C., Petersen, S.L. & Grattan, D.R. Identification of prolactin-sensitive GABA and kisspeptin neurons in regions of the rat hypothalamus involved in the control of fertility. *Endocrinology* **152**, 526-535 (2011).
61. Hodson, D.J., Townsend, J. & Tortonese, D.J. Characterization of the Effects of Prolactin in Gonadotroph Target Cells1. *Biology of Reproduction* **83**, 1046-1055 (2010).
62. Tortonese, D.J., Brooks, J., Ingleton, P.M. & McNeilly, A.S. Detection of prolactin receptor gene expression in the sheep pituitary gland and visualization of the specific translation of the signal in gonadotrophs. *Endocrinology* **139**, 5215-5223 (1998).
63. Henderson, H.L., Townsend, J. & Tortonese, D.J. Direct effects of prolactin and dopamine on the gonadotroph response to GnRH. *J Endocrinol* **197**, 343-350 (2008).
64. Woodside, C. & Jans, J.E. Role of the nutritional status of the litter and length and frequency of mother-litter contact bouts in prolonging lactational diestrus in rats. *Horm Behav* **29**, 154-176 (1995).
65. Liu, X. & Herbison, A.E. Dopamine regulation of gonadotropin-releasing hormone neuron excitability in male and female mice. *Endocrinology* **154**, 340-350 (2013).
66. Greer, M.E., Moraczewski, T. & Rakoff, J.S. Prevalence of hyperprolactinemia in anovulatory women. *Obstetrics and gynecology* **56**, 65-69 (1980).
67. Evans, W., Cronin, M. & Thorner, M. Hypoganadism in hyperprolactinemia: proposed mechanisms. (1982).
68. Koike, K.*, et al.* Effect of prolactin on the secretion of hypothalamic GnRH and pituitary gonadotropins. *Hormone research* **35 Suppl 1**, 5-12 (1991).
69. Patel, S.S. & Bamigboye, V. Hyperprolactinaemia. *Journal of obstetrics and gynaecology : the journal of the Institute of Obstetrics and Gynaecology* **27**, 455-459 (2007).
70. Cohen-Becker, I.R., Selmanoff, M. & Wise, P.M. Hyperprolactinemia alters the frequency and amplitude of pulsatile luteinizing hormone secretion in the ovariectomized rat. *Neuroendocrinology* **42**, 328-333 (1986).
71. Sarkar, D.K. & Yen, S.S. Hyperprolactinemia decreases the luteinizing hormone-releasing hormone concentration in pituitary portal plasma: a possible role for beta-endorphin as a mediator. *Endocrinology* **116**, 2080-2084 (1985).
72. Fox, S.R., Hoefer, M.T., Bartke, A. & Smith, M.S. Suppression of pulsatile LH secretion, pituitary GnRH receptor content and pituitary responsiveness to GnRH by hyperprolactinemia in the male rat. *Neuroendocrinology* **46**, 350-359 (1987).
73. Park, S.K., Keenan, M.W. & Selmanoff, M. Graded hyperprolactinemia first suppresses LH pulse frequency and then pulse amplitude in castrated male rats. *Neuroendocrinology* **58**, 448-453 (1993).
74. Park, S.K. & Selmanoff, M. Dose-dependent suppression of postcastration luteinizing hormone secretion exerted by exogenous prolactin administration in male rats: a model for studying hyperprolactinemic hypogonadism. *Neuroendocrinology* **53**, 404-410 (1991).
75. Grattan, D.R., Jasoni, C.L., Liu, X., Anderson, G.M. & Herbison, A.E. Prolactin regulation of gonadotropin-releasing hormone neurons to suppress luteinizing hormone secretion in mice. *Endocrinology* **148**, 4344-4351 (2007).

Figures

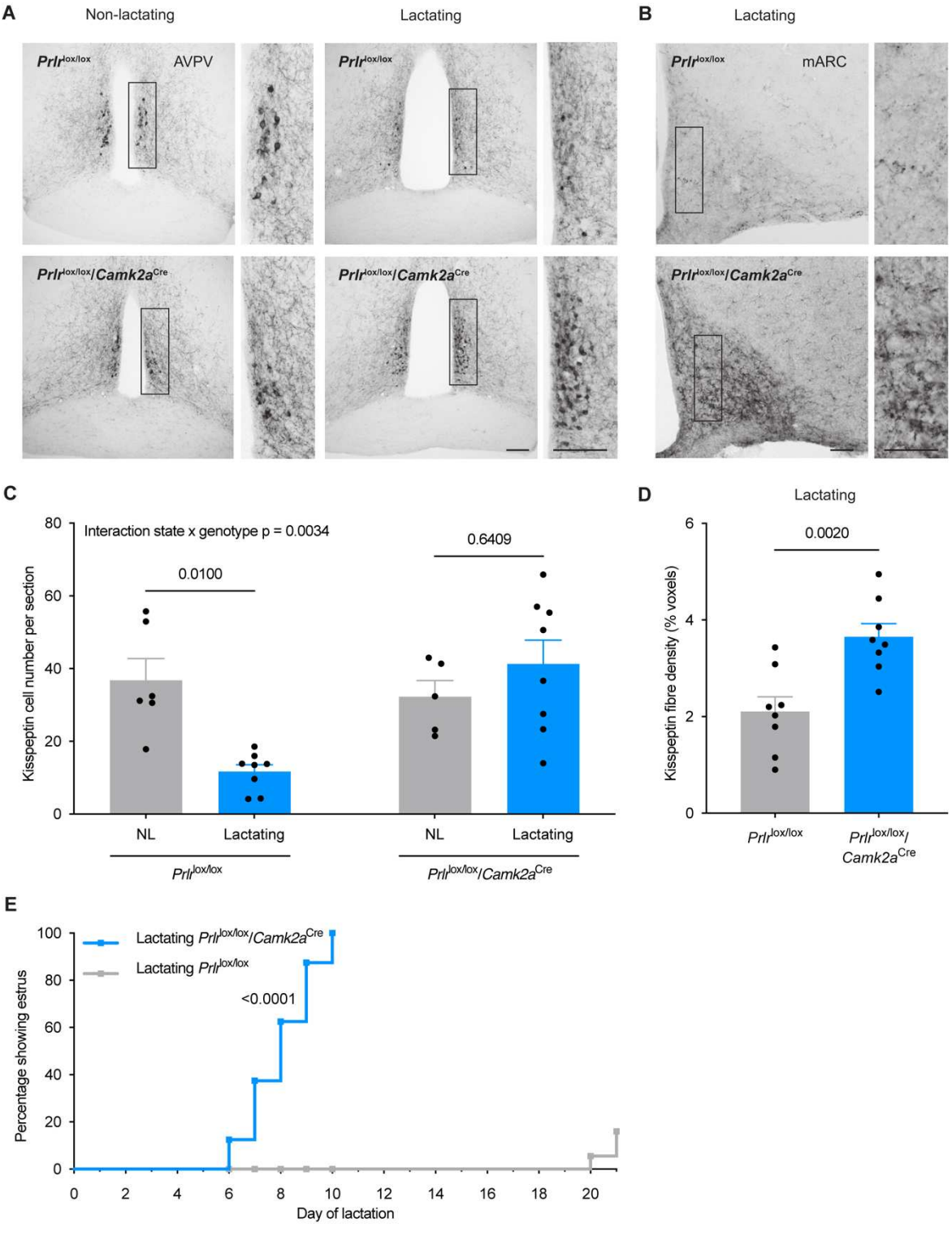

728

729

Figure 1. *Prlr*$^{lox/lox}$/*Camk2a*^{Cre} mice do not undergo the normal period of lactational infertility and the lactation-induced suppression of kisspeptin immunoreactivity is absent. (A) Kisspeptin immunoreactivity shown in representative photomicrographs from the rostral periventricular region of the third ventricle (RP3V) non-lactating (NL; left) and lactating (right) *Prlr*$^{lox/lox}$ control and *Prlr*$^{lox/lox}$/*Camk2a*^{Cre} mice (from anteroventral periventricular nucleus (AVPV) region of RP3V). (B) Representative photomicrographs showing mid arcuate nucleus (mARC) of a lactating *Prlr*$^{lox/lox}$ mouse (top) and a lactating *Prlr*$^{lox/lox}$/*Camk2a*^{Cre} mouse (bottom). (C) Total kisspeptin cell number for the RP3V (NL *Prlr*$^{lox/lox}$ (n = 6) versus lactating *Prlr*$^{lox/lox}$ control (n = 8) p = 0.0100, NL *Prlr*$^{lox/lox}$/*Camk2a*^{Cre} (n = 5) versus lactating *Prlr*$^{lox/lox}$/*Camk2a*^{Cre} (n = 8) p = 0.6409). Two-way ANOVA followed by Tukey's multiple comparisons test. (D) Quantification of kisspeptin fibre density in the arcuate nucleus (Fiji software, measured in percentage voxels per region of interest), showing total kisspeptin fibre density in the arcuate nucleus (lactating *Prlr*$^{lox/lox}$ control n = 8, lactating *Prlr*$^{lox/lox}$/*Camk2a*^{Cre} n = 7, p = 0.0020, unpaired two-tailed t test). (E) *Prlr*$^{lox/lox}$/*Camk2a*^{Cre} mice (blue, n = 8) resume estrous cycles significantly earlier (100% within 6-10 days of lactation) than *Prlr*$^{lox/lox}$ controls (grey, n = 10) (p = <0.0001, Log-rank (Mantel-Cox) test). Scale bar image and insert = 50µm. Values are shown as mean ± SEM.

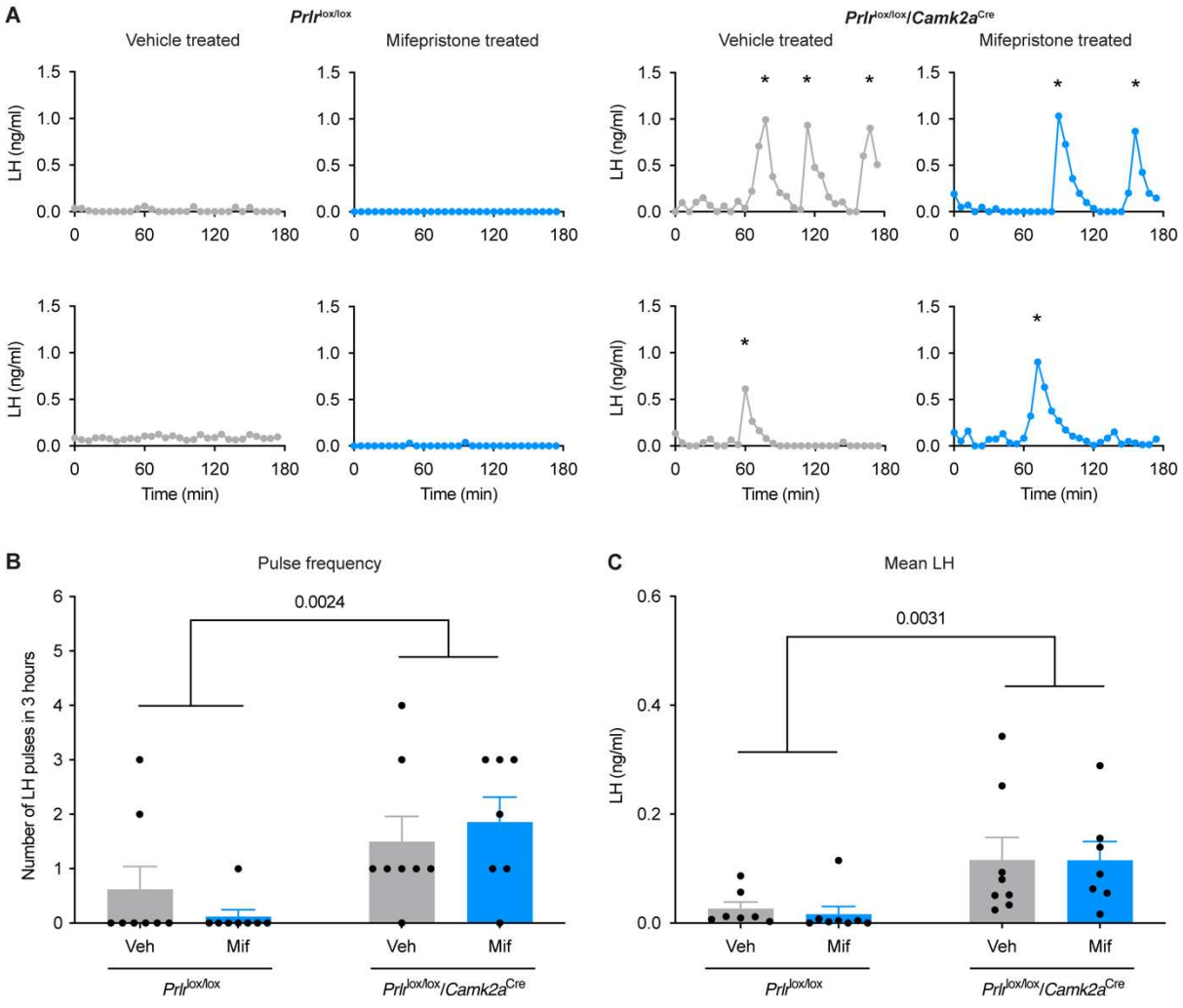

Figure 2. Prolactin action in the brain during lactation is necessary for the suppression of pulsatile LH secretion. Examples of pulsatile LH levels in the blood from lactating *Prlr*$^{lox/lox}$ controls and lactating *Prlr*$^{lox/lox}$/*Camk2a*^{Cre} mice that have either been treated with vehicle (sesame oil, s.c., grey, veh) or 4mg/kg mifepristone (in sesame oil, s.c., blue, mif) on the day prior and on the day of blood sampling (2 injections). Asterisks indicate LH pulse peaks as detected by PULSAR Otago analysis. Graphs show LH pulse frequency (B; interaction p = 0.2807, genotype p = 0.0024, state p = 0.8558), and mean LH levels (C; interaction p = 0.8697, genotype p = 0.0031, state p = 0.8586). Lactating vehicle-treated *Prlr*$^{lox/lox}$ (n = 8), lactating mifepristone-treated *Prlr*$^{lox/lox}$ (n = 8), lactating vehicle-treated *Prlr*$^{lox/lox}$/*Camk2a*^{Cre} (n = 8), lactating mifepristone-treated *Prlr*$^{lox/lox}$/*Camk2a*^{Cre} (n = 7). Two-way ANOVA followed by Tukey's multiple comparisons test. Values are shown as mean ± SEM.

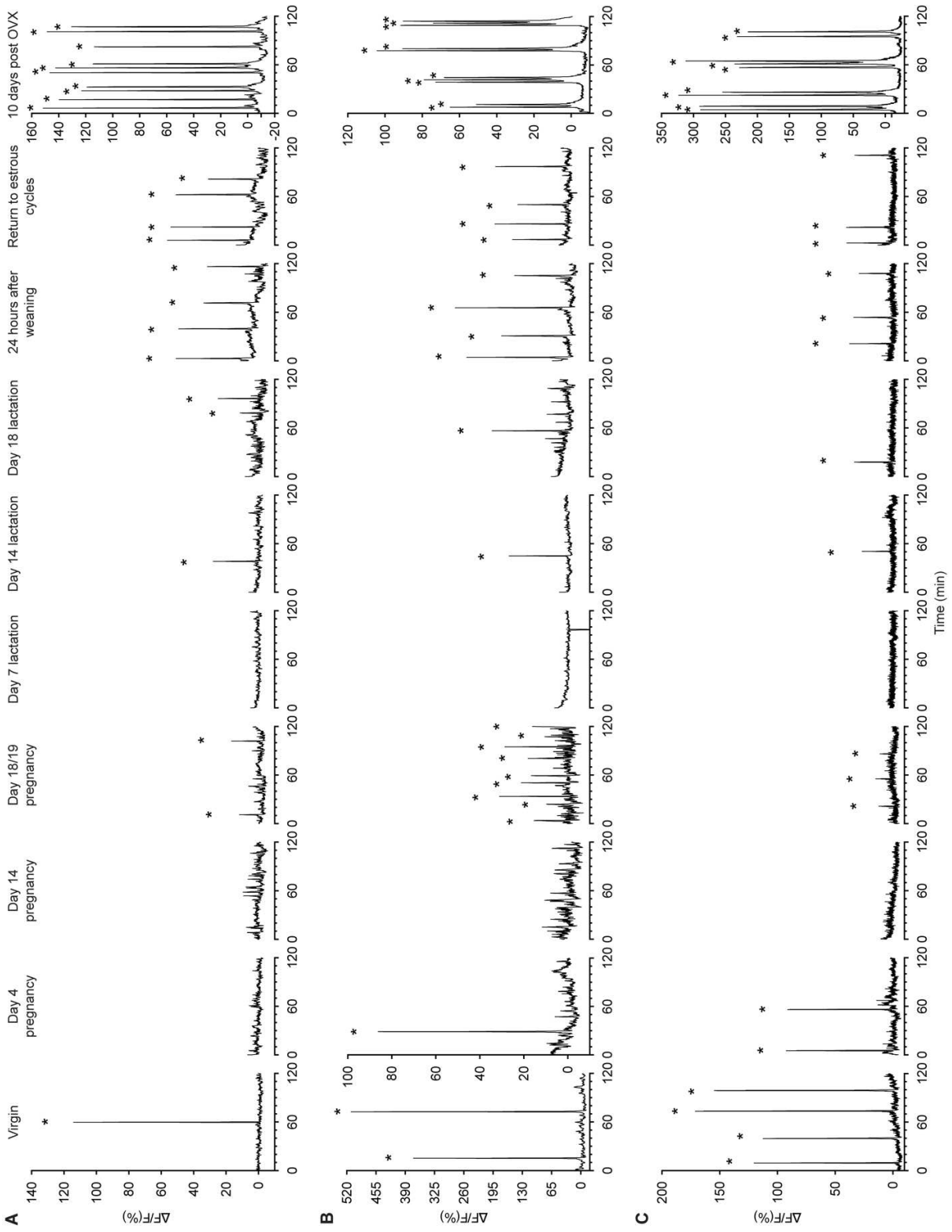

762 **Figure 3. Arcuate kisspeptin neuron GCaMP6 population activity throughout different**
763 **reproductive states in the same mice.** Representative neuronal activity from three *Kiss1*^{Cre}
764 mice throughout the virgin, pregnant, lactating, and post-weaning states. The time points
765 monitored in order were: virgin diestrus, day 4 pregnancy, day 14 pregnancy, day 18/19
766 pregnancy (overnight), day 7 lactation, day 14 lactation, day 18 lactation, 24 hours after
767 weaning (day 22 postpartum), return to normal cycling following weaning (return to estrous
768 cycles), and 10 days post ovariectomy (OVX). Asterisks indicate SEs. Note: dataset from (B)
769 on day 4 of pregnancy onwards and OVX datasets from all mice are on a different y axes
770 scale.

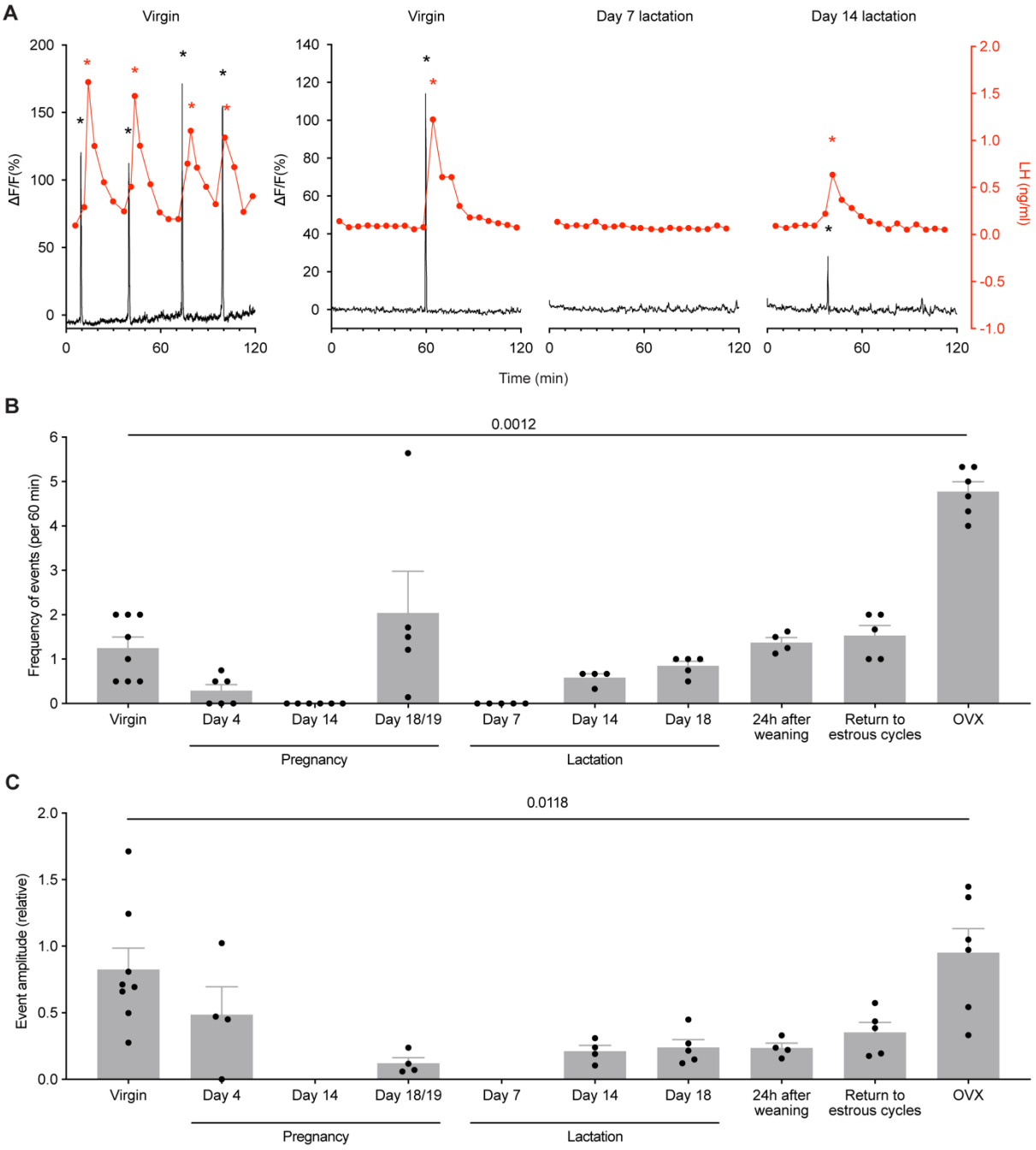

Figure 4. Synchronised Ca^{2+} events are perfectly correlated to pulsatile LH secretion across different reproductive states. (A) When fibre photometry was paired with serial blood sampling for pulsatile LH secretion, the relationship between SEs and LH pulses was examined. Each of the times an SE was seen during a recording with blood sampling, a pulse of LH was also observed, with 100% correlation ($p = <0.0001$, Chi-squared test; 73 out of 73 SEs observed lead to an LH pulse). Representative examples of paired photometry and blood sampling are shown from the diestrous state (virgin), from day 7 lactation where no SEs corresponds with no LH release, and from day 14 lactation when SE are beginning to re-

780 emerge. (B) Quantitative analysis of SE frequency per hour across different reproductive
781 states in *Kiss1*^{Cre} mice ($p = 0.0012$, mixed effect analysis (fixed type III) with Tukey's
782 multiple comparisons tests). (C) Quantitative analysis of SE amplitude of normalised $\Delta F/F$
783 across different reproductive states ($p = 0.0118$, mixed effect analysis (fixed type III) with
784 Tukey's multiple comparisons tests). Black asterisks indicate SEs, red asterisks indicate LH
785 pulse peaks as detected by PULSAR Otago analysis. Values shown as mean ± SEM.

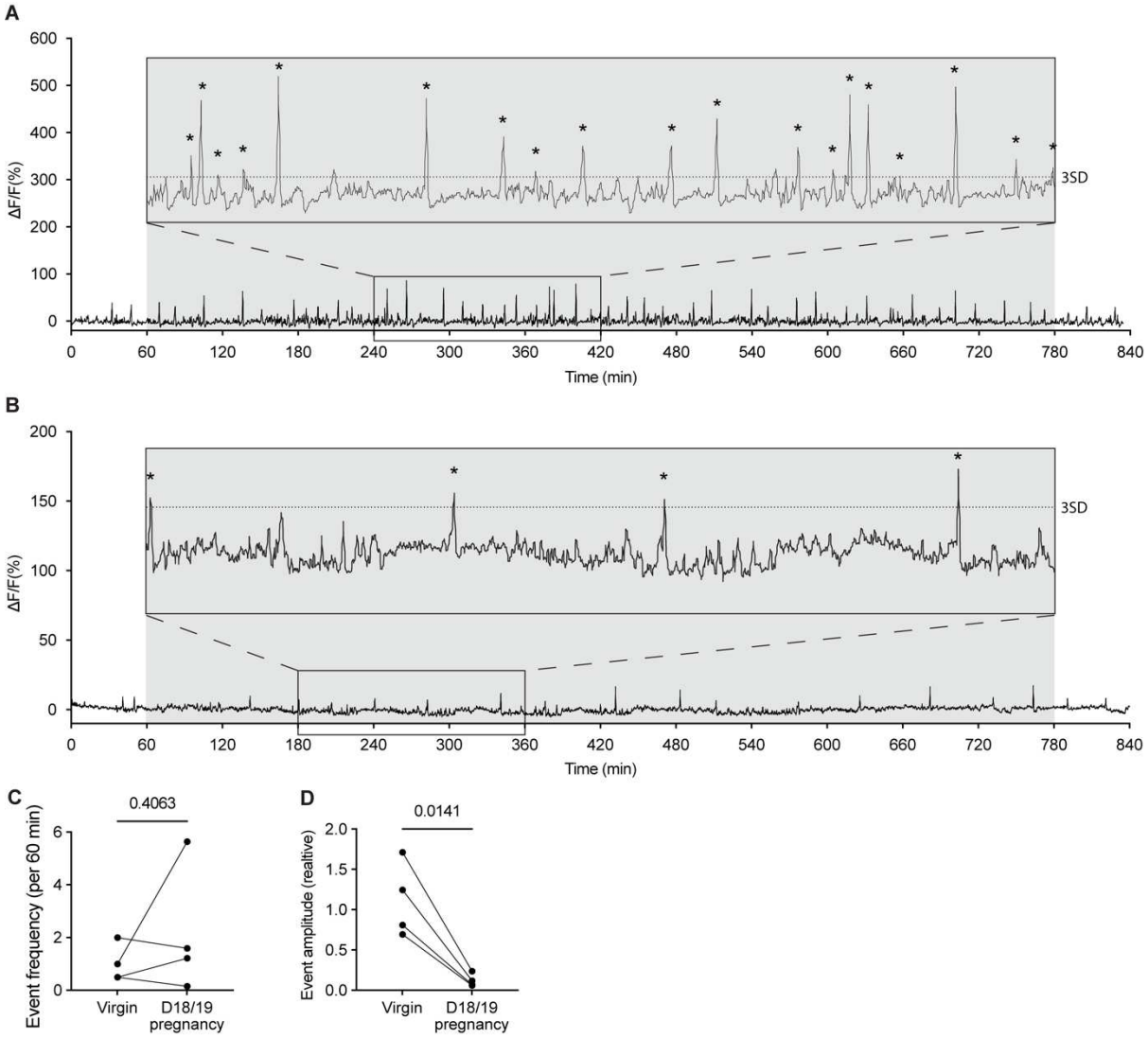

Figure 5. Activity of arcuate kisspeptin neurons on day 18/19 of pregnancy

Fibre photometry recordings of mice on the evening of day 18 of pregnancy (0600 hours) to the morning of day 19 of pregnancy day 19 (0800 hours) shows low amplitude SEs. 3-hour section blown up for ease of viewing. (C) No difference is seen between frequency of SEs (per 60 minutes) in the virgin diestrus versus D18/19 pregnancy ($p = 0.4063$, paired two-tailed t test), however a significant decrease in relative SE amplitude is seen (D; $p = 0.0141$, paired two-tailed t test). Asterisks indicate SEs. Dotted line in insert of (A) and (B) indicates 3 standard deviations (3SD). Grey shaded region = lights off.

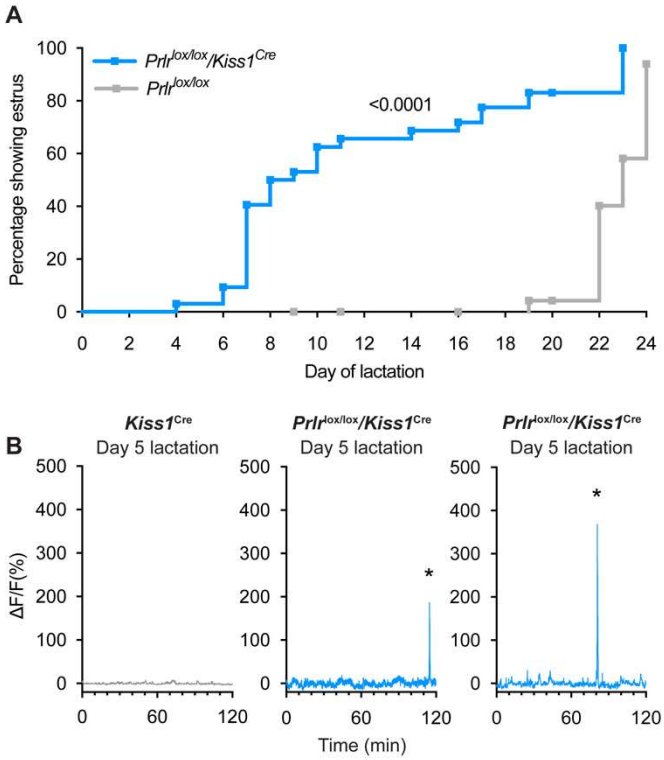

Figure 6. *Prlr*$^{lox/lox}$/*Kiss1*^{Cre} mice do not undergo the normal period of lactational infertility and show early reactivation of arcuate kisspeptin neurons prior to estrus in lactation. (A) *Prlr*$^{lox/lox}$/*Kiss1*^{Cre} mice resume estrous cycles significantly earlier (78% within 4-18 days of lactation, n = 32) than *Prlr*$^{lox/lox}$ controls (0% by day 18, n = 30) (p = <0.0001, Log-rank (Mantel-Cox) test). (B) Representative fibre photometry traces from day 5 of lactation from either a *Kiss1*^{Cre} control mouse or *Prlr*$^{lox/lox}$/*Kiss1*^{Cre} mice. Mice with Prlr knocked out of arcuate kisspeptin neurons (*Prlr*$^{lox/lox}$/*Kiss1*^{Cre}) show SEs early in lactation, which were not seen until day 14 lactation in *Kiss1*^{Cre} control mice. In comparison, the *Kiss1*^{Cre} control mouse shows no SEs, as seen in earlier groups sampled on day 7. Asterisks indicate SEs.

Supplementary data

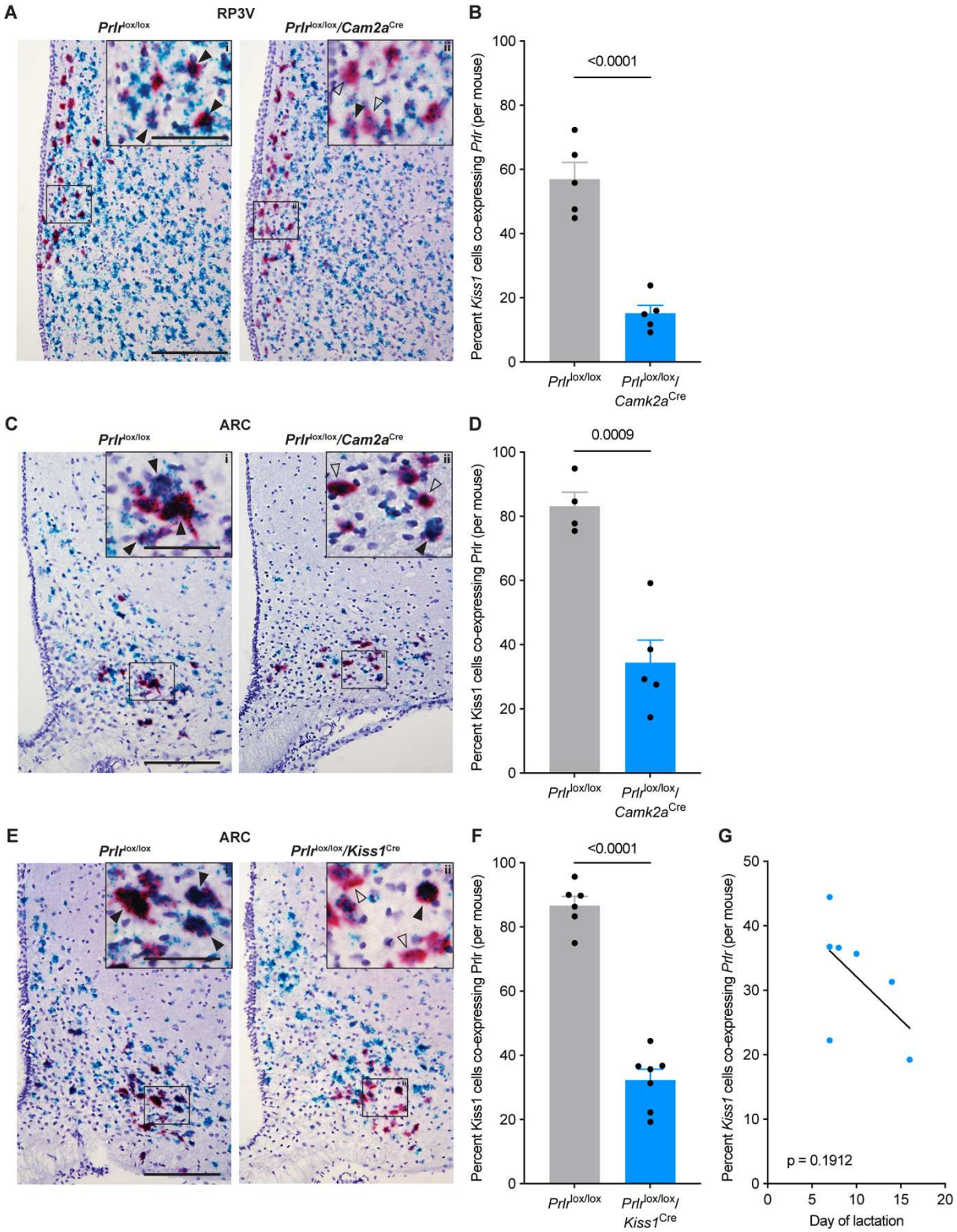

Supplementary Figure 1. Proportion of kisspeptin neurons showing *Prlr* deletion using RNAscope. Representative photomicrographs showing RNAscope labelling for *Prlr* (blue) and *Kiss1* (red) in the rostral periventricular region of the third ventricle (RP3V, A) or arcuate nucleus (ARC, C, E), in either intact ($Prlr^{lox/lox}$ control n = 5, $Prlr^{lox/lox}$/$Camk2a^{Cre}$, n = 5, A) or ovariectomised (OVX; $Prlr^{lox/lox}$ control n = 4, $Prlr^{lox/lox}$/$Camk2a^{Cre}$ n = 5, C; $Prlr^{lox/lox}$ control n = 6, $Prlr^{lox/lox}$/$Kiss1^{Cre}$ n = 7, E) mice. Compared to $Prlr^{lox/lox}$ control mice, $Prlr^{lox/lox}$/$Camk2a^{Cre}$ mice show a significant decrease in percentage of *Kiss1*-expressing cells co-expressing *Prlr* in both the RP3V (B; p = <0.0001) and ARC (D; p = 0.0009) (unpaired two-tailed t tests). (F) A significant decrease in the percent of *Kiss1*-expressing cells co-expressing *Prlr* was seen in $Prlr^{lox/lox}$/$Kiss1^{Cre}$ compared to $Prlr^{lox/lox}$ controls (p = <0.0001, unpaired two-tailed t test). (G) No correlation was found between percentage of *Kiss1* cells co-expressing with *Prlr* and the day of estrus return during lactation (p = 0.1912, simple linear regression). A *Kiss1*-expressing cell was classified as co-expressing *Prlr* mRNA if the density of *Prlr* staining was above background. Solid black arrows = doubled labelled cells expressing both *Kiss1* and *Prlr*; black outlined arrows = *Kiss1* cells with sparse co-labelling for *Prlr*. Scale bar = 150µm, insert = 60µm. Values are shown as mean ± SEM.

826

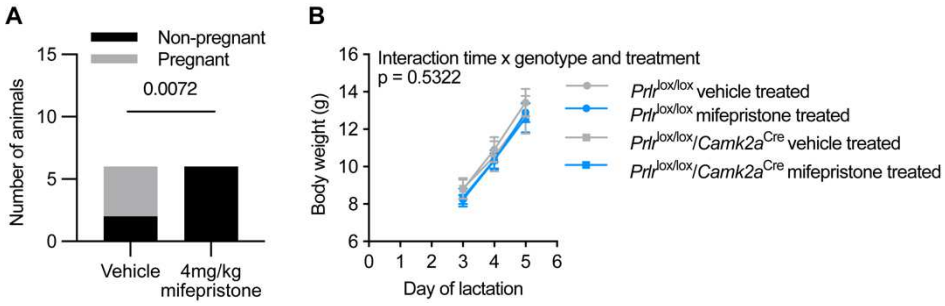

827
828

829

830 **Supplementary Figure 2. Mifepristone dose response and effect on litter weight gain.**
831 (A) Mifepristone dose response trial showing dose of 4mg/kg was sufficient to terminate
832 pregnancy in all mice (p = 0.072, Chi-square test, n = 6 both groups). (B) Mifepristone or
833 vehicle injections had no effect on litter weight gain from day 3 to day 5 of lactation
834 (interaction of time x genotype & treatment p = 0.5322; time p = <0.0001; genotype and
835 treatment p = 0.8811; subject p = <0.0001; two-way ANOVA). Values are shown as mean ±
836 SEM.

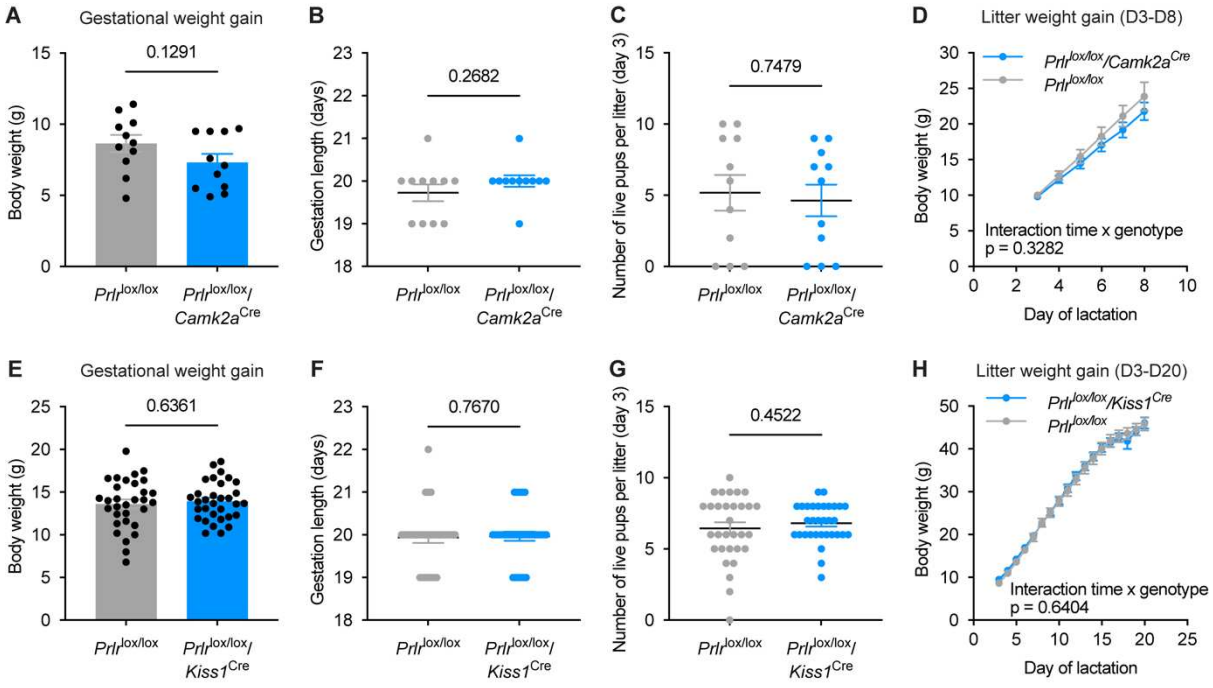

838

839 **Supplementary Figure 3. Gestational and maternal phenotyping of *Prlr*$^{lox/lox}$/*Camk2a*^{Cre}**
840 **and *Prlr*$^{lox/lox}$/*Kiss1*^{Cre} mice and their respective *Prlr*$^{lox/lox}$ controls.** (A-H) Data show
841 gestational weight gain (A; *Prlr*$^{lox/lox}$ n = 11, *Prlr*$^{lox/lox}$/*Camk2a*^{Cre} n = 11; E; *Prlr*$^{lox/lox}$ n = 31,
842 *Prlr*$^{lox/lox}$/*Kiss1*^{Cre} n =27), gestation length (B; *Prlr*$^{lox/lox}$ n = 11, *Prlr*$^{lox/lox}$/*Camk2a*^{Cre} n = 11; F;
843 *Prlr*$^{lox/lox}$ n = 31, *Prlr*$^{lox/lox}$/*Kiss1*^{Cre} n =27), number of live pups on day 3 of lactation (C;
844 *Prlr*$^{lox/lox}$ n = 11; *Prlr*$^{lox/lox}$/*Camk2a*^{Cre} n = 11; G; *Prlr*$^{lox/lox}$ n = 31, *Prlr*$^{lox/lox}$/*Kiss1*^{Cre} n =27),
845 and litter weight gain between day 3-8 of lactation (D; *Prlr*$^{lox/lox}$ n = 8; *Prlr*$^{lox/lox}$/*Camk2a*^{Cre} n
846 = 8) or day 3-20 of lactation (H; *Prlr*$^{lox/lox}$ n = 22, *Prlr*$^{lox/lox}$/*Kiss1*^{Cre} n = 20). There were no
847 differences in any of these parameters (A, C, E, G, unpaired two-tailed t test; B, F, Mann
848 Whitney test; D, H, repeated measures mixed effect analysis, fixed effects (type III) with
849 Šídák's multiple comparisons test. Grey = *Prlr*$^{lox/lox}$; blue A-D = *Prlr*$^{lox/lox}$/*Camk2a*^{Cre,} blue E-
850 H = *Prlr*$^{lox/lox}$/*Kiss1*^{Cre}. Some *Prlr*$^{lox/lox}$ and *Prlr*$^{lox/lox}$/*Kiss1*^{Cre} mice were euthanised prior to
851 day 20 lactation due to COVID-19 lockdown (*Prlr*$^{lox/lox}$ n = 5, *Prlr*$^{lox/lox}$/*Kiss1*^{Cre} n = 5), due to
852 showing estrus and therefore euthanised 2 hours following blood sampling, or when being
853 used as a control for one of these mice (*Prlr*$^{lox/lox}$ n =2, *Prlr*$^{lox/lox}$/*Kiss1*^{Cre} n = 2), or due to a
854 litter losing weight (*Prlr*$^{lox/lox}$ n =1). Values are shown as mean ± SEM.

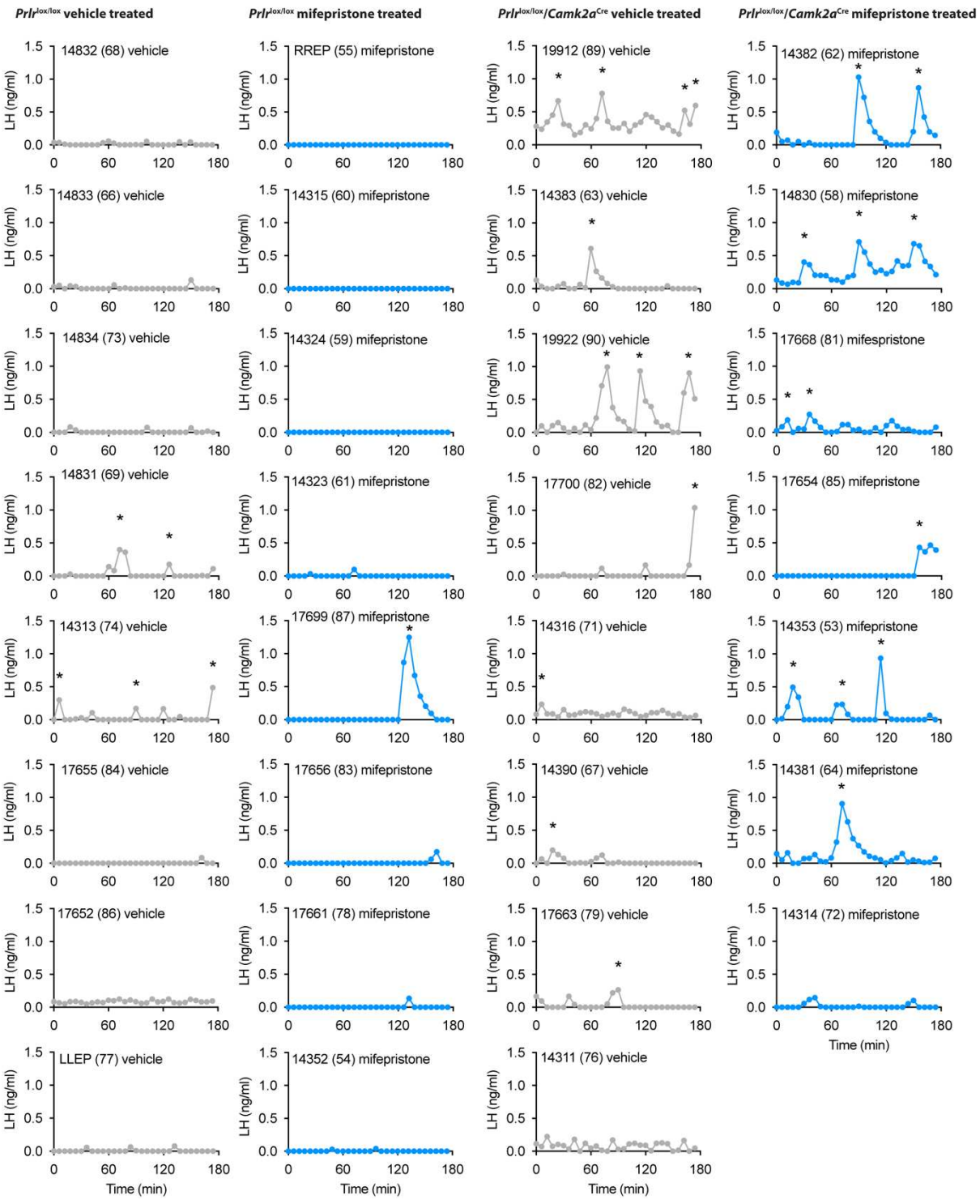

858 **Supplementary Figure 4: Pulsatile LH secretion profiles of *Prlr*$^{lox/lox}$/*Camk2a*^{Cre} mice**
859 **and their controls following vehicle or mifepristone treatment.** Individual LH pulse data
860 from lactating *Prlr*$^{lox/lox}$ controls and *Prlr*$^{lox/lox}$/*Camk2a*^{Cre} mice treated with either vehicle
861 (sesame oil subcutaneous injection, grey) or 4mg/kg mifepristone (in sesame oil
862 subcutaneous injection, blue) once a day for 2 days prior to blood sampling (2 injections).
863 Lactating vehicle-treated *Prlr*$^{lox/lox}$ (n = 8), lactating mifepristone-treated *Prlr*$^{lox/lox}$ (n = 8),
864 lactating vehicle-treated *Prlr*$^{lox/lox}$/*Camk2a*^{Cre} (n = 8), lactating mifepristone-treated
865 *Prlr*$^{lox/lox}$/*Camk2a*^{Cre} (n = 7). Asterisks indicate LH pulse peaks as detected by PULSAR
866 Otago analysis.

867

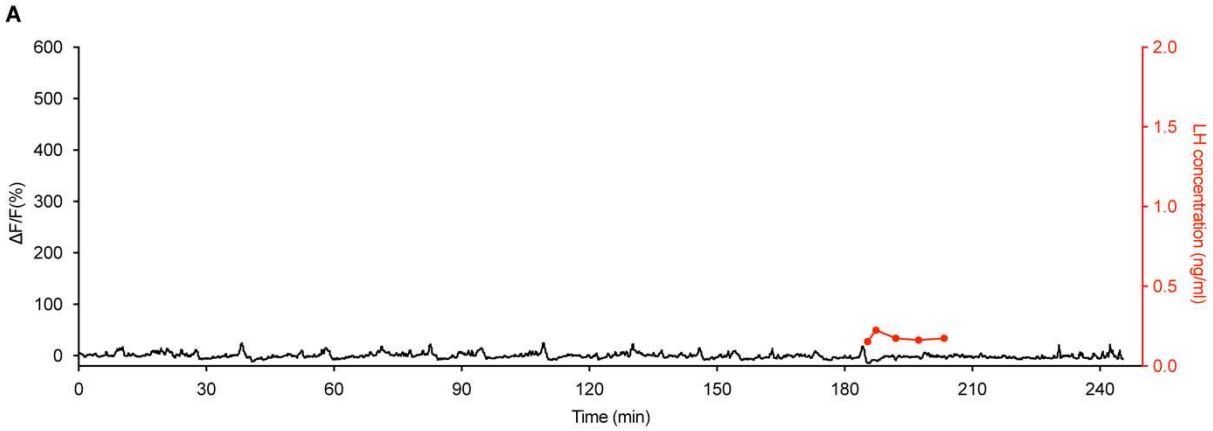

Supplementary Figure 5. Miniature synchronised event-like activity on day 14 of pregnancy does not result in pulsatile LH secretion. (A) Paired fibre photometry and blood sampling from mouse on day 14 of pregnancy showing miniature SE-like activity have no significant effect on pulsatile LH secretion (red).

Supplementary Table 1. Statistics table. Abbreviations for tables below: DF = degrees of freedom; mc = multiple comparison; CI = 95% confidence interval; MW U = Mann Whitney U; MEA = Mixed effect analysis (fixed effects (type III)), RM = repeated measures. Ext = extended data figure.

Fig.	Description	Statistical analysis				
1C	RP3V Kisspeptin immunoreactivity in *Prlr*$^{lox/lox}$/*Camk2a*^{Cre} mice		**p**	**DF**	**CI**	**R^2**
	Interaction	Two-way ANOVA	0.0034	1		
	Genotype	Two-way ANOVA	0.0251	1		
	State	Two-way ANOVA	0.1380	1		
	Prlr$^{lox/lox}$:NL vs. *Prlr*$^{lox/lox}$:Lactating	Tukey's mc	0.0100	23	5.175 to 44.95	
	Prlr$^{lox/lox}$:NL vs. *Prlr*$^{lox/lox}$/*Camk2a*^{Cre}:NL	Tukey's mc	0.9429	23	-17.79 to 26.81	
	Prlr$^{lox/lox}$:NL vs. *Prlr*$^{lox/lox}$/*Camk2a*^{Cre}:Lactating	Tukey's mc	0.9228	23	-24.38 to 15.39	
	Prlr$^{lox/lox}$:Lactating vs. *Prlr*$^{lox/lox}$/*Camk2a*^{Cre}:NL	Tukey's mc	0.0565	23	-41.55 to 0.4412	
	Prlr$^{lox/lox}$:Lactating vs. *Prlr*$^{lox/lox}$/*Camk2a*^{Cre}:Lactating	Tukey's mc	0.0010	23	-47.97 to -11.15	
	Prlr$^{lox/lox}$/*Camk2a*^{Cre}:NL vs. *Prlr*$^{lox/lox}$/*Camk2a*^{Cre}:Lactating	Tukey's mc	0.6409	23	-30.00 to 11.99	
1D	Arcuate Kisspeptin immunoreactivity in *Prlr*$^{lox/lox}$/*Camk2a*^{Cre} mice	Unpaired two-tailed t test	0.0020	14	0.6692 to 2.424	0.5052
1E	*Prlr*$^{lox/lox}$/*Camk2a*^{Cre} do not show lactational diestrus		**p**	**X^2**	**DF**	
	Percent mice showing estrous	Log rank (Mantel-Cox) test	<0.0001	42.37	1	
2B	Effect of mifepristone treatment on LH pulse frequency in *Prlr*$^{lox/lox}$/*Camk2a*^{Cre} mice		**p**	**DF**	**CI**	
	Interaction	Two-way ANOVA	0.2807	1		
	Genotype	Two-way ANOVA	0.0024	1		
	Treatment	Two-way ANOVA	0.8558	1		
	Prlr$^{lox/lox}$:Veh vs. *Prlr*$^{lox/lox}$:Mif	Tukey's mc	0.7922	27	-0.9804 to 1.980	
	Prlr$^{lox/lox}$:Veh vs. *Prlr*$^{lox/lox}$/*Camk2a*^{Cre}:Veh	Tukey's mc	0.3861	27	-2.355 to 0.6054	
	Prlr$^{lox/lox}$:Veh vs. *Prlr*$^{lox/lox}$/*Camk2a*^{Cre}:Mif	Tukey's mc	0.1487	27	-2.765 to 0.3002	
	Prlr$^{lox/lox}$:Mif vs. *Prlr*$^{lox/lox}$/*Camk2a*^{Cre}:Veh	Tukey's mc	0.0758	27	-2.765 to 0.3002	
	Prlr$^{lox/lox}$:Mif vs. *Prlr*$^{lox/lox}$/*Camk2a*^{Cre}:Mif	Tukey's mc	0.0223	27	-2.765 to 0.3002	
	Prlr$^{lox/lox}$/*Camk2a*^{Cre}:Veh vs. *Prlr*$^{lox/lox}$/*Camk2a*^{Cre}:Mif	Tukey's mc	0.9188	27	-1.890 to 1.175	
2C	Effect of mifepristone treatment on mean LH in *Prlr*$^{lox/lox}$/*Camk2a*^{Cre} mice		**p**	**DF**		
	Interaction	Two-way ANOVA	0.8697	1		
	Genotype	Two-way ANOVA	0.0031	1		
	Treatment	Two-way ANOVA	0.8586	1		
	Prlr$^{lox/lox}$:Veh vs. *Prlr*$^{lox/lox}$:Mif	Tukey's mc	0.9947	26	-0.1021 to 0.1220	
	Prlr$^{lox/lox}$:Veh vs. *Prlr*$^{lox/lox}$/*Camk2a*^{Cre}:Veh	Tukey's mc	0.1528	26	-0.2015 to 0.02263	

Fig.	Description	Statistical analysis				
	$Prlr^{lox/lox}$:Veh vs. $Prlr^{lox/lox}/Camk2a^{Cre}$:Mif	Tukey's mc	0.1765	26	-0.2047 to 0.02672	
	$Prlr^{lox/lox}$:Mif vs. $Prlr^{lox/lox}/Camk2a^{Cre}$:Veh	Tukey's mc	0.0803	26	-0.2076 to 0.008853	
	$Prlr^{lox/lox}$:Mif vs. $Prlr^{lox/lox}/Camk2a^{Cre}$:Mif	Tukey's mc	0.0974	26	-0.2110 to 0.01306	
	$Prlr^{lox/lox}/Camk2a^{Cre}$:Veh vs. $Prlr^{lox/lox}/Camk2a^{Cre}$:Mif	Tukey's mc	>0.9999	26	-0.1116 to 0.1125	
4B	Kisspeptin activity across different reproductive states		**p**	**DF**	**CI**	
	Event frequency across states	MEA	0.0012			
	Virgin vs. Day 4 pregnancy	Tukey's mc	0.0828	5	-0.1356 to 2.052	
	Virgin vs. Day 14 pregnancy	Tukey's mc	0.0586	5	-0.05175 to 2.552	
	Virgin vs. Day 18/19 pregnancy	Tukey's mc	0.9837	4	-5.518 to 3.932	
	Virgin vs. Day 7 lactation	Tukey's mc	0.0912	4	-0.2517 to 2.752	
	Virgin vs. Day 14 lactation	Tukey's mc	0.6584	3	-1.598 to 2.931	
	Virgin vs. Day 18 lactation	Tukey's mc	0.9638	4	-1.661 to 2.461	
	Virgin vs. 24h after weaning	Tukey's mc	>0.9999	3	-3.097 to 2.847	
	Virgin vs. Return to estrous cycles	Tukey's mc	0.9993	4	-3.016 to 2.449	
	Virgin vs. OVX	Tukey's mc	0.0009	5	-4.955 to -2.100	
	Day 4 pregnancy vs. Day 14 pregnancy	Tukey's mc	0.5635	5	-0.3793 to 0.9626	
	Day 4 pregnancy vs. Day 18/19 pregnancy	Tukey's mc	0.6960	4	-6.958 to 3.455	
	Day 4 pregnancy vs. Day 7 lactation	Tukey's mc	0.6396	4	-0.5180 to 1.101	
	Day 4 pregnancy vs. Day 14 lactation	Tukey's mc	0.4286	3	-1.026 to 0.4430	
	Day 4 pregnancy vs. Day 18 lactation	Tukey's mc	0.2948	4	-1.579 to 0.4622	
	Day 4 pregnancy vs. 24h after weaning	Tukey's mc	0.1309	3	-2.649 to 0.4820	
	Day 4 vs. Return to estrous cycles	Tukey's mc	0.1986	4	-3.185 to 0.7012	
	Day 4 pregnancy vs. OVX	Tukey's mc	<0.0001	5	-5.683 to -3.290	
	Day 14 pregnancy vs. Day 18/19 pregnancy	Tukey's mc	0.5272	4	-7.022 to 2.936	
	Day 14 pregnancy vs. Day 7 lactation	Tukey's mc				
	Day 14 pregnancy vs. Day 14 lactation	Tukey's mc	0.0343	3	-1.092 to -0.07436	
	Day 14 pregnancy vs. Day 18 lactation	Tukey's mc	0.0092	4	-1.380 to -0.3202	
	Day 14 pregnancy vs. 24h after weaning	Tukey's mc	0.0072	3	-2.072 to -0.6781	
	Day 14 pregnancy vs. Return to estrous cycles	Tukey's mc	0.0210	4	-2.731 to -0.3355	
	Day 14 pregnancy vs. OVX	Tukey's mc	<0.0001	5	-5.877 to -3.679	
	Day 18/19 pregnancy vs. Day 7 lactation	Tukey's mc	0.6053	3	-4.432 to 8.518	
	Day 18/19 pregnancy vs. Day 14 lactation	Tukey's mc	0.9434	2	-11.74 to 14.66	
	Day 18/19 pregnancy vs. Day 18 lactation	Tukey's mc	0.9458	3	-5.853 to 8.239	
	Day 18/19 pregnancy vs. 24h after weaning	Tukey's mc	0.9807	2	-6.951 to 8.287	
	Day 18/19 pregnancy vs. Return to estrous cycles	Tukey's mc	0.9952	3	-4.164 to 5.183	
	Day 18/19 pregnancy vs. OVX	Tukey's mc	0.2556	4	-7.450 to 1.980	
	Day 7 lactation vs. Day 14 lactation	Tukey's mc	0.0382	3	-1.112 to -0.05439	
	Day 7 lactation vs. Day 18 lactation	Tukey's mc	0.0325	3	-1.578 to -0.1222	
	Day 7 lactation vs. 24h after weaning	Tukey's mc	0.0412	2	-2.620 to -0.1304	
	Day 7 lactation vs. Return to estrous cycles	Tukey's mc	0.0514	3	-3.083 to 0.01609	
	Day 7 lactation vs. OVX	Tukey's mc	0.0002	4	-5.887 to -3.669	

Fig.	Description	Statistical analysis				
	Day 14 lactation vs. Day 18 lactation	Tukey's mc	0.8130	3	-1.405 to 0.8715	
	Day 14 lactation vs. 24h after weaning	Tukey's mc	0.1642	2	-2.285 to 0.7020	
	Day 14 lactation vs. Return to estrous cycles	Tukey's mc	0.2736	2	-3.366 to 1.466	
	Day 14 lactation vs. OVX	Tukey's mc	0.0026	3	-5.734 to -2.655	
	Day 18 lactation vs. 24h after weaning	Tukey's mc	0.1662	3	-1.362 to 0.3122	
	Day 18 lactation vs. Return to estrous cycles	Tukey's mc	0.1946	3	-1.849 to 0.4823	
	Day 18 lactation vs. OVX	Tukey's mc	0.0016	4	-5.475 to -2.380	
	24h after weaning vs. Return to estrous cycles	Tukey's mc	0.9643	3	-1.180 to 0.8630	
	24h after weaning vs. OVX	Tukey's mc	0.0080	3	-5.192 to -1.614	
	Return to estrous cycles vs OVX	Tukey's mc	0.0113	4	-5.382 to -1.107	
4C	Kisspeptin activity across different reproductive states		**p**	**DF**	**CI**	
	Event amplitude across states	MEA	0.0118			
	Virgin vs. Day 4	Tukey's mc	0.7336	3	-0.9745 to 1.654	
	Virgin vs. Day 18/19	Tukey's mc	0.2608	3	-0.6762 to 2.086	
	Virgin vs. Day 14	Tukey's mc	0.0851	3	-0.1362 to 1.365	
	Virgin vs. Day 18	Tukey's mc	0.1766	4	-0.2966 to 1.467	
	Virgin vs. 24h after weaning	Tukey's mc	0.4700	3	-0.9997 to 2.178	
	Virgin vs. Return to estrous cycles	Tukey's mc	0.4514	4	-0.5997 to 1.546	
	Virgin vs. OVX	Tukey's mc	0.9938	5	-0.9886 to 0.7359	
	Day 4 vs. Day 18/19	Tukey's mc	0.7336	1	-5.882 to 6.612	
	Day 4 vs. Day 14	Tukey's mc	0.7858	2	-1.431 to 1.981	
	Day 4 vs. Day 18	Tukey's mc	0.6250	2	-0.9138 to 1.405	
	Day 4 vs. 24h after weaning	Tukey's mc	0.2399	1	-0.8660 to 1.365	
	Day 4 vs. Return to estrous cycles	Tukey's mc	0.9217	2	-1.026 to 1.293	
	Day 4 vs. OVX	Tukey's mc	0.5530	3	-1.870 to 0.9381	
	Day 18/19 vs. Day 14	Tukey's mc	0.7069	2	-0.5763 to 0.3960	
	Day 18/19 vs. Day 18	Tukey's mc	0.1985	3	-0.3267 to 0.08725	
	Day 18/19 vs. 24h after weaning	Tukey's mc	0.6222	2	-0.6603 to 0.4286	
	Day 18/19 vs. Return to estrous cycles	Tukey's mc	0.2384	2	-0.7754 to 0.3120	
	Day 18/19 vs. OVX	Tukey's mc	0.1494	3	-2.103 to 0.4405	
	Day 14 vs. Day 18	Tukey's mc	0.9929	3	-0.3118 to 0.2526	
	Day 14 vs. 24h after weaning	Tukey's mc	0.5747	2	-0.1375 to 0.08624	
	Day 14 vs. Return to estrous cycles	Tukey's mc	0.4210	2	-0.6226 to 0.3396	
	Day 14 vs. OVX	Tukey's mc	0.3306	3	-2.375 to 0.8931	
	Day 18 vs. 24h after weaning	Tukey's mc	>0.9999	3	-0.3977 to 0.4056	
	Day 18 vs. Return to estrous cycles	Tukey's mc	0.6644	3	-0.5038 to 0.2799	
	Day 18 vs. OVX	Tukey's mc	0.1809	4	-1.793 to 0.3702	
	24h after weaning vs. Return to estrous cycles		0.5101	3	-0.4457 to 0.2140	
	24h after weaning vs. OVX	Tukey's mc	0.2874	3	-2.185 to 0.7540	
	Return to estrous cycles vs. OVX	Tukey's mc	0.2096	4	-1.563 to 0.3637	
5C	Virgin vs day 18/19 pregnancy frequency of events		**p**	**R^2**	**CI**	
		Paired two-tailed t test	0.4063	0.2364	-2.646 to 4.945	
5D	Virgin vs day 18/19 pregnancy relative event amplitude		**p**	**R^2**	**CI**	
		Paired two-tailed t test	0.0141	0.8989	-1.606 to -0.3816	
6A	*Prlr*$^{lox/lox}$/*Kiss1*^{Cre} do not show lactational diestrus		**p**	**X^2**	**DF**	
	Percent mice showing estrus	Log rank (Mantel-Cox) test	<0.0001	38.02	1	
Ext 1A-D	*Prlr*$^{lox/lox}$/*Camk2a*^{Cre} maternal and gestational phenotyping		**p**	**R^2**	**CI**	**MW U**
	A: gestational weight gain	Unpaired two-tailed t test	0.1291	0.1113	-3.076 to 0.4219	
	B: gestation length	Mann Whitney test	0.2682			45.50

Fig.	Description	Statistical analysis				
	C: number of live pups	Unpaired two-tailed t test	0.7479	0.005282	-4.037 to 2.946	
	D: litter weight gain					
	Time	MEA	<0.0001			
	Genotype	MEA	0.3833			
	Time x genotype	MEA	0.3282			
	Day 3 lactation	Šídák's mc	>0.9999		-3.740 to 4.115	
	Day 4 lactation	Šídák's mc	0.9993		-3.365 to 4.490	
	Day 5 lactation	Šídák's mc	0.9863		-2.965 to 4.890	
	Day 6 lactation	Šídák's mc	0.9525		-2.690 to 5.165	
	Day 7 lactation	Šídák's mc	0.6938		-1.953 to 5.903	
	Day 8 lactation	Šídák's mc	0.619		-1.821 to 6.112	
Ext1 E-H	*Prlr*$^{lox/lox}$/*Kiss1*^{Cre} maternal and gestational phenotyping		**p**	**R^2**	**CI**	**MW U**
	E: gestational weight gain	Unpaired two-tailed t test	0.6361	0.003694	-0.9985 to 1.622	
	F: gestation length	Mann Whitney test	0.7670			471.5
	G: number of live pups	Unpaired two-tailed t test	0.4522	0.009296	-0.5930 to 1.315	
	H: litter weight gain					
	Time x Genotype	Two-way RM ANOVA	0.6404			
	Time	Two-way RM ANOVA	<0.0001			
	Genotype	Two-way RM ANOVA	0.9014			
	Subject	Two-way RM ANOVA	<0.0001			
	Day 3 lactation	Šídák's mc	>0.9999		-5.407 to 3.653	
	Day 4 lactation	Šídák's mc	>0.9999		-5.204 to 3.857	
	Day 5 lactation	Šídák's mc	>0.9999		-5.159 to 3.902	
	Day 6 lactation	Šídák's mc	>0.9999		-5.105 to 3.956	
	Day 7 lactation	Šídák's mc	>0.9999		-4.976 to 4.084	
	Day 8 lactation	Šídák's mc	>0.9999		-4.226 to 4.834	
	Day 9 lactation	Šídák's mc	>0.9999		-4.757 to 4.304	
	Day 10 lactation	Šídák's mc	>0.9999		-4.650 to 4.410	
	Day 11 lactation	Šídák's mc	>0.9999		-5.154 to 3.907	
	Day 12 lactation	Šídák's mc	>0.9999		-5.242 to 3.819	
	Day 13 lactation	Šídák's mc	>0.9999		-4.936 to 4.125	
	Day 14 lactation	Šídák's mc	>0.9999		-4.979 to 4.081	
	Day 15 lactation	Šídák's mc	>0.9999		-4.776 to 4.284	
	Day 16 lactation	Šídák's mc	>0.9999		-4.152 to 4.909	
	Day 17 lactation	Šídák's mc	>0.9999		-4.216 to 4.845	
	Day 18 lactation	Šídák's mc	0.9912		-2.717 to 6.343	
	Day 19 lactation	Šídák's mc	>0.9999		-4.182 to 4.878	
	Day 20 lactation	Šídák's mc	>0.9999		-4.752 to 4.309	
Ext 3	Proportion of kisspeptin neurons showing *Prlr* deletion using RNAscope		**p**	**R^2**	**CI**	
	B: *Prlr*$^{lox/lox}$/*Camk2a*^{Cre} RP3V	Unpaired two-tailed t test	<0.0001	0.8740	-55.02 to 28.69	
	D: *Prlr*$^{lox/lox}$/*Camk2a*^{Cre} ARC	Unpaired two-tailed t test	0.0009	0.8123	-69.72 to 8.860	
	F: *Prlr*$^{lox/lox}$/*Kiss1*^{Cre} ARC	Unpaired two-tailed t test	<0.0001	0.9300	-64.27 to -44.46	
	G: correlation of day of estrus and average density of *Prlr* on *Kiss1*-expressing cells (per animal)	Simple linear regression	0.1912	0.3135		
Ext 4A	Mifepristone functional dose response trial		**p**	**X^2**	**Z**	
		Chi-square test	0.0072	6	2.449	
Ext 4B	Mifepristone has no effect on litter weight gain		**p**	**DF**		
	Time x Genotype and treatment	Two-way RM ANOVA	0.5322	6		
	Time	Two-way RM ANOVA	<0.0001	2		
	Genotype and treatment	Two-way RM ANOVA	0.8811	3		

Fig.	Description	Statistical analysis				
	Subject	Two-way RM ANOVA	<0.0001	22		

877